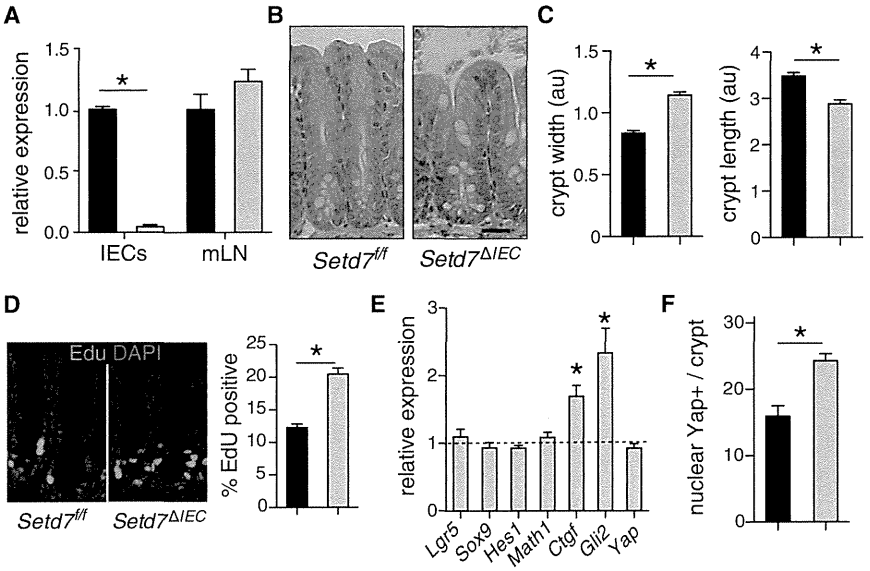

Figure 1. IEC-Intrinsic Expression of Set7 Controls Intestinal Homeostasis

(A) *Setd7*$^{f/f}$ (black bars) and *Setd7*$^{\Delta IEC}$ (gray bars) IECs and mesenteric lymph nodes (mLN) were isolated from *Setd7*$^{f/f}$ and *Setd7*$^{\Delta IEC}$ mice. *Setd7* expression, relative to that in *Setd7*$^{f/f}$ mice, was assessed by qPCR.

(B) H&E stained section of cecal tissue. Bar, 25 μm.

(C) Quantification of crypt width and length (50 crypts per mouse, five mice per group).

(D) Representative cecal section stained for EdU and DAPI. Frequency of EdU-positive cells per crypt is shown in graph (40 crypts per mouse from five mice).

(E) Expression of indicated genes in IECs isolated from naive *Setd7*$^{f/f}$ and *Setd7*$^{\Delta IEC}$ mice was determined by qPCR. Expression is relative to *Setd7*$^{f/f}$ IECs using actin as housekeeping gene.

(F) Cecal sections were analyzed by immunofluorescent staining for Yap. The number of nuclei per crypt that exhibited characteristic speckled nuclear localization of Yap is shown (50 crypts per mouse from five mice per group). Data are presented as mean ± SEM (n = 5–10 mice per genotype).

au, arbitrary units. *$p < 0.05$. See also Figure S1.

deficient in Set7, we demonstrate that Set7 is a central component of the Hippo pathway through the regulation of Yap localization. We show that Yap and Set7 interact, that Yap is monomethylated at K494, and that a mutated Yap (Yap^{K494R}) is not cytoplasmically retained. Taken together, our results identify a methylation-dependent checkpoint in the Hippo pathway that may act as a therapeutic target to modulate this pathway.

RESULTS AND DISCUSSION

To directly assess the cell autonomous role of Set7 in vivo, we generated intestinal epithelial cell (IEC)-specific Set7-deficient mice (*Setd7*$^{\Delta IEC}$ mice) by crossing mice in which exon 2 was flanked with loxP sites (*Setd7*$^{f/f}$ mice) with mice expressing the Cre recombinase under the control of the IEC-specific *Villin* promoter (el Marjou et al., 2004; Lehnertz et al., 2011). *Setd7*$^{\Delta IEC}$ mice lack *Setd7* expression specifically in IECs (Figure 1A) and display no overt phenotypes. However, examination of the intestines of *Setd7*$^{\Delta IEC}$ mice revealed differences in the intestinal architecture compared to that of control *Setd7*$^{f/f}$ mice. Intestinal crypts from *Setd7*$^{\Delta IEC}$ mice were shorter and wider than those of *Setd7*$^{f/f}$ mice (Figures 1B and 1C). We also observed an increased frequency of proliferating cells per crypt in *Setd7*$^{\Delta IEC}$ mice (Figure 1D), as measured by examining cellular uptake of EdU 2 hr following injection. IEC proliferation and differentiation are tightly regulated processes controlled by the Wnt, Notch, and Hippo signaling pathways (Cai et al., 2010; Camargo et al., 2007; van der Flier and Clevers, 2009). We isolated IECs from colons of naive *Setd7*$^{f/f}$ and *Setd7*$^{\Delta IEC}$ mice and measured gene expression of direct and indirect target genes of the different pathways. Wnt (*Lgr5* and *Sox9*) and Notch (*Hes1* and *Math1*) target genes were not differentially expressed in IECs isolated from naive *Setd7*$^{\Delta IEC}$ mice compared to *Setd7*$^{f/f}$ mice (Figure 1E). In contrast, Hippo pathway-associated genes *Ctgf* and *Gli2* were expressed at significantly higher levels in IECs isolated from *Setd7*$^{\Delta IEC}$ mice (Figure 1E), suggesting a cell-intrinsic role for Set7 in regulating Hippo pathway-associated genes.

In wild-type mice, protein expression of the Hippo transducer Yap is only observed in the nuclei of cells at the base of the intestinal crypt and is associated with intestinal stem cells and transit-amplifying progenitor cells (Cai et al., 2010; Camargo et al., 2007). Consistent with increased expression of Yap target genes in IECs from *Setd7*$^{\Delta IEC}$ mice, we observed significantly increased numbers of Yap-positive nuclei per crypt in *Setd7*$^{\Delta IEC}$ mice compared to *Setd7*$^{f/f}$ mice, with differences being most notable in the upper half of the crypt (Figure 1F; Figure S1 available online). From these data, we conclude that IEC-intrinsic expression of Set7 is required to regulate the size of the proliferative progenitor compartment, potentially through regulation of the Hippo pathway. Of note, a previous study has shown that mice with an IEC-intrinsic deletion of the upstream Hippo pathway adaptor protein Salvador1/WW45 (*Sav1*) also had wider and shorter crypts with more proliferative progenitors (Cai et al., 2010).

To directly test whether Set7 was directly involved in regulation of the Hippo pathway, we studied the well-described Hippo-pathway-dependent process, cell-cell contact-mediated growth inhibition (Zhao et al., 2007). We used immortalized MEFs derived from *Setd7*$^{-/-}$ and *Setd7*$^{+/+}$ mice (Lehnertz et al., 2011). Although no difference in proliferation was detected in the first 48 hr after seeding, once cells reached confluence, *Setd7*$^{-/-}$ MEFs were less susceptible to contact inhibition of proliferation than *Setd7*$^{+/+}$ MEFs as indicated by increasing cell number over time (Figure 2A). Although we failed to detect any differences in expression of the canonical Yap target genes *Ctgf* and *Cdc20* in low-density *Setd7*$^{+/+}$ or *Setd7*$^{-/-}$ MEFs, we observed significantly increased expression of *Ctgf* and *Cdc20* in high-density *Setd7*$^{-/-}$ MEFs compared to *Setd7*$^{+/+}$ MEFs (Figure 2B). Furthermore, *Setd7* expression was not affected by cell density and *Yap* expression was similar in *Setd7*$^{+/+}$ or

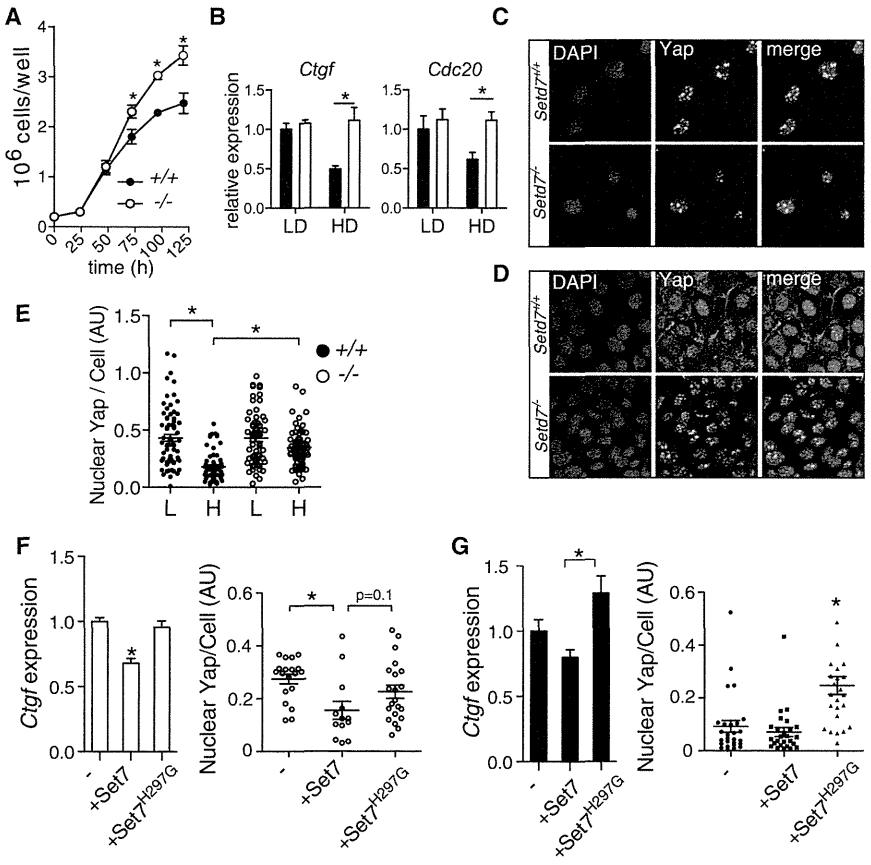

Figure 2. Set7 Regulates Cell-Cell Contact-Mediated Growth Inhibition, and Set7 Methyltransferase Activity Is Required for Yap Localization and Function

(A) *Setd7*$^{+/+}$ (closed circles) and *Setd7*$^{-/-}$ (open circles) MEFs were plated at 2 × 10^5 cells per well, and cell numbers were counted at various time points after plating.

(B) Expression of Yap-dependent genes in low-density (LD) and high-density (HD) *Setd7*$^{+/+}$ (closed bars) and *Setd7*$^{-/-}$ (open bars) MEFs was determined by qPCR. Expression is relative to *Setd7*$^{+/+}$ using actin as housekeeping gene.

(C and D) Yap localization in (C) low-density and (D) high-density *Setd7*$^{+/+}$ and *Setd7*$^{-/-}$ MEFs was determined by immunofluorescent staining.

(E) Nuclear Yap was quantified for individual nuclei of *Setd7*$^{+/+}$ (closed circles) and *Setd7*$^{-/-}$ (open circles) MEFs. L, low-density cultures; H, high-density cultures.

(F) *Setd7*$^{-/-}$ MEFs were transfected with plasmids expressing either Set7 or methyltransferase-deficient Set7^{H297G} and expression of *Ctgf* and Yap localization was determined.

(G) *Setd7*$^{+/+}$ MEFs were transfected with plasmids expressing either Set7 or methyltransferase-deficient Set7^{H297G} and expression of *Ctgf* and Yap localization was determined. Data are mean ± SEM and are representative of two to four independent experiments.

AU, arbitrary units. *p < 0.05. See also Figure S2.

Setd7$^{-/-}$ MEFs at low or high density (Figure S2A). This suggests that Set7 is required for downregulation of Yap-dependent genes in contact-inhibited MEFs.

Yap activity is regulated by cytoplasmic retention and proteasomal degradation, both of which are regulated by phosphorylation (Zhao et al., 2010; Zhao et al., 2007). In low-density cultures, Yap was localized in the nucleus in both *Setd7*$^{+/+}$ and *Setd7*$^{-/-}$ MEFs (Figures 2C and 2E). Consistent with previous studies (Schlegelmilch et al., 2011; Zhao et al., 2007), we observed translocation of Yap to the cytosol and cytoplasmic membrane in high-density cultures of *Setd7*$^{+/+}$ MEFs (Figures 2D and 2E). Strikingly, in high-density *Setd7*$^{-/-}$ MEFs, Yap remained primarily in the nucleus (Figures 2D and 2E), consistent with the increased expression of Yap-dependent genes. Thus, these results demonstrate that Set7 is required for the correct subcellular localization of Yap following cell-cell contact.

Since KMTs can have methyltransferase-independent functions (Lehnertz et al., 2010; Purcell et al., 2011), we next examined whether Yap regulation by Set7 was methyltransferase dependent. We transfected *Setd7*$^{+/+}$ and *Setd7*$^{-/-}$ MEFs with wild-type Set7 or a mutant form of Set7 with a point mutation of residue 297 histidine to a glycine (Set7^{H297G}) that has been shown to inactivate the methyltransferase activity (Nishioka et al., 2002; Tao et al., 2011), and we measured *Ctgf* expression and nuclear Yap. In *Setd7*$^{-/-}$ MEFs, we were able to recover both *Ctgf* gene expression and loss of nuclear Yap (Figure 2F) with Set7 but not Set7^{H297G}, indicating that the methyltransferase activity of Set7 is required for the cytoplasmic retention of Yap and subsequent regulation of target genes. As part of our control experiments, we also transfected the plasmids into *Setd7*$^{+/+}$ MEFs. Strikingly, we found that Set7^{H297G} acts as a dominant negative, as the introduction of this construct in *Setd7*$^{+/+}$ MEFs resulted in increased *Ctgf* expression and enhanced nuclear Yap (Figure 2G). Thus, the methyltransferase activity of Set7 is a critical regulatory mechanism that controls the Hippo pathway through the subcellular localization of Yap.

Following phosphorylation of Yap, two distinct processes—cytoplasmic retention and ubiquitin-mediated degradation—are initiated (Zhao et al., 2010). Although we did not detect cytoplasmic Yap in high-density *Setd7*$^{-/-}$ MEFs by immunofluorescence, we failed to observe a difference in the levels of S127-phosphorylated Yap in *Setd7*$^{+/+}$ and *Setd7*$^{-/-}$ MEFs (Figure 3A), demonstrating that, in the absence of Set7, Yap can exit the nucleus and be phosphorylated but that cytoplasmic retention is impaired. We next tested if degradation of Yap was impaired. To test this, we seeded equal numbers of *Setd7*$^{+/+}$ and *Setd7*$^{-/-}$ MEFs cells at low and high densities by varying the size of the culture dish. Twenty-four hours later, we observed similar density-induced degradation of Yap (Figure 3B), demonstrating that the degradation pathway was not impaired in the absence of Set7. Furthermore, when we left high-density cultures to overgrow for an additional 48 hr, we observed reduced total Yap levels in *Setd7*$^{-/-}$ MEFs compared to *Setd7*$^{+/+}$ MEFs (Figure 3C), suggesting that cytoplasmic retention and not degradation was impaired in the absence of Set7. Consistent with this, confocal microscopy of the overgrown (hyperconfluent) cells

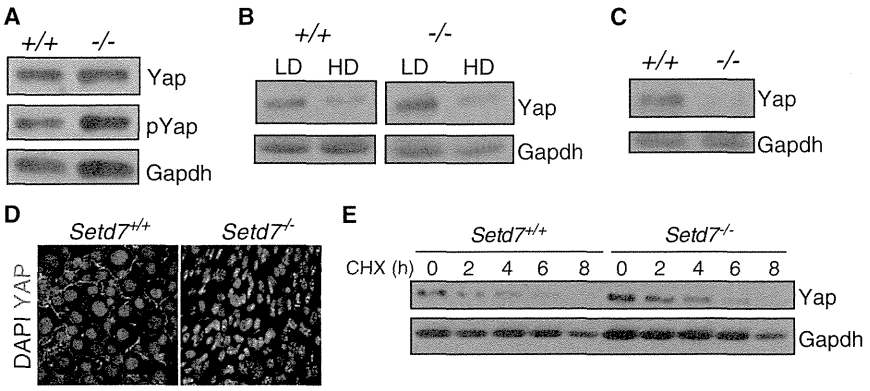

Figure 3. Set7 Does Not Control Phosphorylation or Degradation of Yap

(A) *Setd7*$^{+/+}$ or *Setd7*$^{-/-}$ MEFs were grown to confluence, and whole cell extracts were immunoblotted with antibodies against Yap, pYap S127, and Gapdh.

(B) Equal cell numbers were seeded in either a petri dish or six-well plate and lysed 24 hr later. Density-dependent Yap degradation was not affected by lack of Set7.

(C and D) High-density seeded cells were overgrown for an additional 48 hr (hyperconfluent), and Yap was (C) quantified and (D) localized.

(E) Kinetics of Yap degradation was determined by treating *Setd7*$^{+/+}$ and *Setd7*$^{-/-}$ MEFs with cycloheximide (CHX) for indicated hours, followed by immunoblotting of whole cell extracts with antibodies against Yap and Gapdh. Results are representative of more than three independent experiments.

revealed that Yap accumulates in the cytoplasm/membrane of *Setd7*$^{+/+}$ MEFs, whereas the remaining Yap in *Setd7*$^{-/-}$ MEFs was primarily nuclear (Figure 3D). Finally, to test degradation kinetics, we incubated high-density *Setd7*$^{+/+}$ and *Setd7*$^{-/-}$ MEFs in the presence of cycloheximide and followed Yap protein levels over time. We did not observe differences in the degradation kinetics of Yap between *Setd7*$^{+/+}$ and *Setd7*$^{-/-}$ MEFs (Figure 3E). Having a fully functional degradation pathway is the likely reason *Setd7*$^{-/-}$ mice are viable, and we do not observe a phenotype similar to mice that overexpress Yap or YapS127A (Camargo et al., 2007; Dong et al., 2007). Together, these results indicate that Set7 is required for cytoplasmic retention, but not degradation, of Yap.

To determine how Set7 regulates Yap localization, we examined whether Set7 interacted with Yap. Coimmunoprecipitation of native Yap from *Setd7*$^{+/+}$ MEFs cultured at high density demonstrated that Set7 was in a complex with Yap (Figure 4A), but not with Tead1 (Figure S3A). Because Set7 does not have a signal sequence to enter or leave the nucleus (Donlin et al., 2012), we hypothesized that Set7-Yap interactions were occurring in the cytoplasm. We found that Set7, like pYapS127, was present primarily in the cytoplasm of high-density (confluent) MEFs (Figure 4B), suggesting that Set7 binds Yap in the cytoplasm and that this is where Set7 likely acts to promote the cytoplasmic retention of Yap. When immunoprecipitated Yap was analyzed by immunoblotting with two distinct anti-methyl lysine antibodies (ab23366, recognizing both mono- and dimethylated lysine, and ab7315, recognizing primarily dimethylated lysine) we found that Yap was monomethylated in *Setd7*$^{+/+}$ MEFs but not in *Setd7*$^{-/-}$ MEFs (Figure 4A). These results, combined with our finding that Set7 forms complexes with Yap, suggested that Set7 could directly monomethylate Yap.

Mass spectrometric analysis of Yap immunoprecipitated from confluent HEK293 cells stably expressing a Flag-tagged version of Yap was performed. Targeted high-resolution multiple reaction monitoring of the Yap 488-498 peptide revealed that a single lysine residue (K494) is monomethylated (Figure 4C), consistent with the monomethyltransferase activity of Set7 (Xiao et al., 2003). Di- or trimethylation of Yap K494 could not be detected (Table S1). To directly test whether K494 was involved in the subcellular localization of Yap, we transfected *Setd7*$^{+/+}$ MEFs with Yap containing either a mutation of the methylation site K494 (K494R) or the adjacent lysine residue K497 (K497R). Strikingly, we observed increased Yap nuclear localization in MEFs transfected with Yap K494R but not K497R (Figures 4D and 4E), despite normal S127 phosphorylation (Figure 4G). We observed increased *Ctgf* expression in cells transfected with the YapK494R mutant (Figure 4F). Although we cannot unequivocally rule out other potential methylation sites in Yap, our results indicate that monomethylation of Yap specifically at K494 is required for Yap cytoplasmic retention and function.

In this study, we have identified several phenotypes in *Setd7*$^{-/-}$ mice that suggest the involvement of Set7 in regulation of the Hippo pathway. One observation from our studies is that Set7 is a cytoplasmic protein in high-density grown MEFs, which could explain the normal levels of H3K4me1 observed in *Setd7*$^{-/-}$ MEFs (Lehnertz et al., 2011). Unlike most KMTs, Set7 does not have a nuclear export signal or nuclear localization signal (Donlin et al., 2012), and Set7 is the only methyltransferase that contains membrane occupation and recognition nexus repeats (Morn repeats) that are found in proteins linking the membrane to the cytoskeleton (Garbino et al., 2009). It is tempting to speculate that Set7 is located at cellular junctions where it would methylate and sequester Yap from nuclear entry and degradation. While phosphorylation of Yap by the upstream Hippo pathway kinases Lats1/2 has been shown to regulate cytoplasmic retention, our results demonstrate that Set7 is critical for the cytoplasmic sequestration of Yap through the monomethylation of K494. The molecular mechanisms of how Yap methylation controls cytoplasmic sequestration are unknown. The K494 methylation site in Yap is proximal to the carboxyl-terminal PDZ-binding domain, and methylation of this site may impinge upon Yap interactions with PDZ-dependent binding partners including Zona occludens-2 (Oka et al., 2010) and Nherf (Mohler et al., 1999). Furthermore, methylated Yap is a minority of the total cellular Yap protein, suggesting that Yap methylation is a dynamic process, and future studies to identify specific demethylases potentially involved in Yap localization are warranted. Finally, whether Hippo-pathway-dependent phosphorylation of Yap is required for Set7-dependent methylation remains

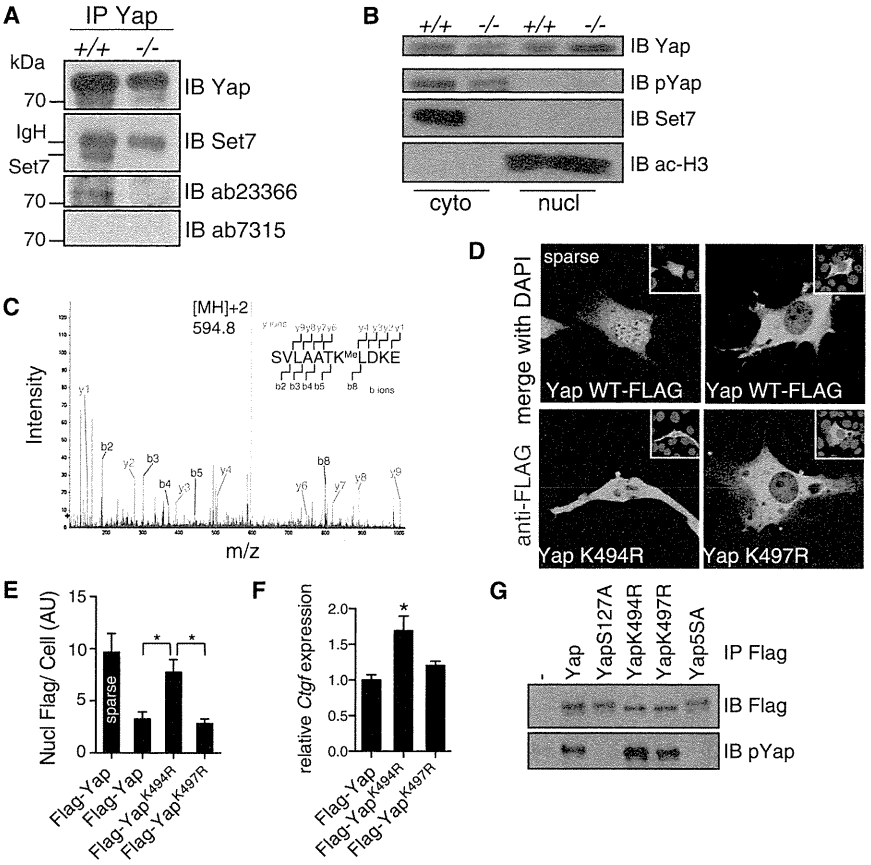

Figure 4. Set7 Monomethylates Yap on Lysine 494, and Lysine 494 Is Required for Cytoplasmic Retention

(A) Anti-Yap immunoprecipitates (IP) from high-density *Setd7*$^{+/+}$ and *Setd7*$^{-/-}$ MEFs were immunoblotted for Yap, Set7, methyl-lysine (mono-, dimethylated) (ab23366), and dimethyl-lysine (ab7315). IB, immunoblots.

(B) Cytosolic and nuclear fractions were isolated from high-density (confluent) cell cultures and probed for Yap, pYap, Set7, and Histone H3.

(C) Tandem mass spectrometry spectrum of Glu-C-digested Yap488-498 fragment (methylated K494 [MH]+2, mass 594.8 Da). Detected product ions are indicated in red (y ions) and blue (b ions).

(D) *Setd7*$^{+/+}$ MEFs were transfected with indicated Flag-Yap constructs, grown to confluence (unless indicated), and stained with a Flag-specific antibody followed by a fluorescent secondary antibody and DAPI.

(E) Nuclear Flag fluorescence was quantified.

(F) *Setd7*$^{+/+}$ MEFs were transfected with indicated plasmids, and *Ctgf* expression was measured of confluent cell cultures.

(G) HEK293 cells were transfected with indicated constructs, anti-Flag was used for IP, and IPs were immunoblotted using anti-Flag and anti-pYapS127. Data are presented as mean ± SEM and are representative of two to three experiments.

au, arbitrary units. *p < 0.05. See also Figure S3 and Table S1.

an open question. More generally, our finding that methylation is an important mechanism for controlling cytoplasmic/nuclear localization could have implications for other proteins that are regulated by subcellular localization.

EXPERIMENTAL PROCEDURES

Mice

Villin-Cre mice were obtained from Jackson Laboratories. *Setd7*$^{-/-}$ and *Setd7*$^{f/f}$ mice were described previously (Lehnertz et al., 2011). We did not observe any physiological effects from Cre expression. Animals were maintained in a specific-pathogen-free environment and tested negative for pathogens in routine screening. All experiments were carried out at the University of British Columbia following institutional guidelines.

IEC Isolation

IECs were isolated as previously described (Zaph et al., 2007). Briefly, intestines were opened lengthwise, washed in PBS containing penicillin and streptomycin, and cut into 1 cm pieces. IECs were obtained by shaking intestinal tissue in 2 mM EDTA in PBS for 20 min at 37°C twice. IECs were isolated, RNA was purified, and gene expression analyzed by quantitative PCR (qPCR).

Tissue Staining

Large intestines were fixed in formalin and paraffin-embedded. Tissue sections were stained with hematoxylin and eosin (H&E). Slides were analyzed on a Zeiss Axioplan2 microscope, and images were captured using a Qimaging Retiga EX CCD camera and Openlab 4.0.4 software (PerkinElmer). For immunofluorescence, 5 μm sections of paraformaldehyde-fixed, paraffin-embedded tissues were incubated with anti-Yap (Cell Signaling) followed by Alexa568-conjugated goat anti-rabbit and DAPI. Mice were injected with EdU 2 hr prior to sacrifice, and cecal sections were stained using Alexa568 Azide (Invitrogen) according to manufacturer instructions.

Cell Culture, Proliferation, and Transfection

MEFs were isolated and immortalized with SV40 as described previously (Lehnertz et al., 2011), and they were cultured in Dulbecco's modified Eagle's medium (DMEM) containing 10% fetal calf serum (FCS) and antibiotics, detached using trypsin (0.25%), and seeded at appropriate densities. Cells were counted after trypsin detachment using a hemocytometer. MEFs were transfected with plasmids encoding Flag-Set7, Flag-Set7^{H297G} (a point mutation that abolishes Set7 methyltransferase activity) (Nishioka et al., 2002; Tao et al., 2011), Flag-Yap, Flag-Yap^{K494R}, or Flag-Yap^{K497R} (Addgene "19045") (Oka et al., 2008; Hata et al., 2012) constructs using Lipofectamine 2000 (Invitrogen) according to the manufacturer's descriptions.

Yap Localization

Cells were seeded at different densities on tissue-culture-treated plastic chamber slides (ibidi GmbH) in DMEM + 10% FCS and incubated for 24 hr. Cells were then fixed in 4% paraformaldehyde for 20 min, permeabilized in 0.5% Triton X in PBS for 3 min, and blocked in 3% bovine serum albumin (BSA) in PBS for 20 min. Fixed cells were incubated with rabbit anti-Yap antibodies (Cell Signaling) in 3% BSA in PBS at a dilution of 1:200 for 40 min, washed five times for 5 min with PBS, and then incubated with secondary Alexa 488/568-conjugated goat anti-rabbit antibodies at a dilution of 1:400 for 20 min. Cells were again washed five times for 5 min with PBS, and then mounting media that contained DAPI (Invitrogen) was added before imaging with a confocal microscope (Olympus FV1000).

Statistical Analysis

Results represent the mean ± SEM. Statistical significance was determined by Student's t test or one-way analysis of variance with subsequent post hoc test.

SUPPLEMENTAL INFORMATION

Supplemental Information includes Supplemental Experimental Procedures, three figures, and one table and can be found with this article online at http://dx.doi.org/10.1016/j.devcel.2013.05.025.

ACKNOWLEDGMENTS

This work was supported by the Canadian Institutes of Health Research (CIHR; grants MSH-95368, MOP-89773, and MOP-106623 to C.Z., MOP-123433 to A.-C.G., and grant MOP-68865 to M.R.G.) and a Canada Foundation for Innovation grant (to C.Z.). The Structural Genomics Consortium is a registered charity (number 1097737) that receives funds from AbbVie, Boehringer Ingelheim, Canada Foundation for Innovation, the Canadian Institutes for Health Research (CIHR), Genome Canada through the Ontario Genomics Institute (OGI-055), GlaxoSmithKline, Janssen, Lilly Canada, the Novartis Research Foundation, the Ontario Ministry of Economic Development and Innovation, Pfizer, Takeda, and the Wellcome Trust (092809/Z/10/Z). The development of the mouse strains used in this study was supported by funds from the Leon Judah Blackmore Foundation (to F.M.V.R.). S.A.F. was supported by fellowships from the CIHR and the Michael Smith Foundation for Health Research (MSFHR). F.A. is the recipient of a CIHR/Canadian Association of Gastroenterologists (CAG)/Crohn's and Colitis Foundation of Canada postdoctoral fellowship. M.J.O. is the recipient of a CIHR/CAG/Janssen postdoctoral fellowship. C.H.A. holds a Canada Research Chair in Structural Genomics. F.M.V.R. is a Distinguished Scholar in Residence of the Peter Wall Institute for Advanced Studies. C.Z. is a CIHR New Investigator and an MSFHR Career Investigator.

Received: December 17, 2012
Revised: April 24, 2013
Accepted: May 28, 2013
Published: July 11, 2013

REFERENCES

Cai, J., Zhang, N., Zheng, Y., de Wilde, R.F., Maitra, A., and Pan, D. (2010). The Hippo signaling pathway restricts the oncogenic potential of an intestinal regeneration program. Genes Dev. *24*, 2383–2388.

Camargo, F.D., Gokhale, S., Johnnidis, J.B., Fu, D., Bell, G.W., Jaenisch, R., and Brummelkamp, T.R. (2007). YAP1 increases organ size and expands undifferentiated progenitor cells. Curr. Biol. *17*, 2054–2060.

Campaner, S., Spreafico, F., Burgold, T., Doni, M., Rosato, U., Amati, B., and Testa, G. (2011). The methyltransferase Set7/9 (Setd7) is dispensable for the p53-mediated DNA damage response *in vivo*. Mol. Cell *43*, 681–688.

Chuikov, S., Kurash, J.K., Wilson, J.R., Xiao, B., Justin, N., Ivanov, G.S., McKinney, K., Tempst, P., Prives, C., Gamblin, S.J., et al. (2004). Regulation of p53 activity through lysine methylation. Nature *432*, 353–360.

Cordenonsi, M., Zanconato, F., Azzolin, L., Forcato, M., Rosato, A., Frasson, C., Inui, M., Montagner, M., Parenti, A.R., Poletti, A., et al. (2011). The Hippo transducer TAZ confers cancer stem cell-related traits on breast cancer cells. Cell *147*, 759–772.

Dong, J., Feldmann, G., Huang, J., Wu, S., Zhang, N., Comerford, S.A., Gayyed, M.F., Anders, R.A., Maitra, A., and Pan, D. (2007). Elucidation of a universal size-control mechanism in *Drosophila* and mammals. Cell *130*, 1120–1133.

Donlin, L.T., Andresen, C., Just, S., Rudensky, E., Pappas, C.T., Kruger, M., Jacobs, E.Y., Unger, A., Zieseniss, A., Dobenecker, M.W., et al. (2012). Smyd2 controls cytoplasmic lysine methylation of Hsp90 and myofilament organization. Genes Dev. *26*, 114–119.

Ea, C.K., and Baltimore, D. (2009). Regulation of NF-kappaB activity through lysine monomethylation of p65. Proc. Natl. Acad. Sci. USA *106*, 18972–18977.

el Marjou, F., Janssen, K.P., Chang, B.H., Li, M., Hindie, V., Chan, L., Louvard, D., Chambon, P., Metzger, D., and Robine, S. (2004). Tissue-specific and inducible Cre-mediated recombination in the gut epithelium. Genesis *39*, 186–193.

Estève, P.O., Chin, H.G., Benner, J., Feehery, G.R., Samaranayake, M., Horwitz, G.A., Jacobsen, S.E., and Pradhan, S. (2009). Regulation of DNMT1 stability through SET7-mediated lysine methylation in mammalian cells. Proc. Natl. Acad. Sci. USA *106*, 5076–5081.

Garbino, A., van Oort, R.J., Dixit, S.S., Landstrom, A.P., Ackerman, M.J., and Wehrens, X.H. (2009). Molecular evolution of the junctophilin gene family. Physiol. Genomics *37*, 175–186.

Hata, S., Hirayama, J., Kajiho, H., Nakagawa, K., Hata, Y., Katada, T., Furutani-Seiki, M., and Nishina, H. (2012). A novel acetylation cycle of transcription co-activator Yes-associated protein that is downstream of Hippo pathway is triggered in response to SN2 alkylating agents. J. Biol. Chem. *287*, 22089–22098.

Heallen, T., Zhang, M., Wang, J., Bonilla-Claudio, M., Klysik, E., Johnson, R.L., and Martin, J.F. (2011). Hippo pathway inhibits Wnt signaling to restrain cardiomyocyte proliferation and heart size. Science *332*, 458–461.

Huang, J., and Berger, S.L. (2008). The emerging field of dynamic lysine methylation of non-histone proteins. Curr. Opin. Genet. Dev. *18*, 152–158.

Jenuwein, T., and Allis, C.D. (2001). Translating the histone code. Science *293*, 1074–1080.

Kanai, F., Marignani, P.A., Sarbassova, D., Yagi, R., Hall, R.A., Donowitz, M., Hisaminato, A., Fujiwara, T., Ito, Y., Cantley, L.C., and Yaffe, M.B. (2000). TAZ: a novel transcriptional co-activator regulated by interactions with 14-3-3 and PDZ domain proteins. EMBO J. *19*, 6778–6791.

Kouskouti, A., Scheer, E., Staub, A., Tora, L., and Talianidis, I. (2004). Gene-specific modulation of TAF10 function by SET9-mediated methylation. Mol. Cell *14*, 175–182.

Krummel, K.A., Lee, C.J., Toledo, F., and Wahl, G.M. (2005). The C-terminal lysines fine-tune P53 stress responses in a mouse model but are not required for stability control or transactivation. Proc. Natl. Acad. Sci. USA *102*, 10188–10193.

Kurash, J.K., Lei, H., Shen, Q., Marston, W.L., Granda, B.W., Fan, H., Wall, D., Li, E., and Gaudet, F. (2008). Methylation of p53 by Set7/9 mediates p53 acetylation and activity in vivo. Mol. Cell *29*, 392–400.

Lehnertz, B., Northrop, J.P., Antignano, F., Burrows, K., Hadidi, S., Mullaly, S.C., Rossi, F.M., and Zaph, C. (2010). Activating and inhibitory functions for the histone lysine methyltransferase G9a in T helper cell differentiation and function. J. Exp. Med. *207*, 915–922.

Lehnertz, B., Rogalski, J.C., Schulze, F.M., Yi, L., Lin, S., Kast, J., and Rossi, F.M. (2011). p53-dependent transcription and tumor suppression are not affected in Set7/9-deficient mice. Mol. Cell *43*, 673–680.

Mohler, P.J., Kreda, S.M., Boucher, R.C., Sudol, M., Stutts, M.J., and Milgram, S.L. (1999). Yes-associated protein 65 localizes p62(c-Yes) to the apical compartment of airway epithelia by association with EBP50. J. Cell Biol. *147*, 879–890.

Nishioka, K., Chuikov, S., Sarma, K., Erdjument-Bromage, H., Allis, C.D., Tempst, P., and Reinberg, D. (2002). Set9, a novel histone H3 methyltransferase that facilitates transcription by precluding histone tail modifications required for heterochromatin formation. Genes Dev. *16*, 479–489.

Oka, T., Mazack, V., and Sudol, M. (2008). Mst2 and Lats kinases regulate apoptotic function of Yes kinase-associated protein (YAP). J. Biol. Chem. *283*, 27534–27546.

Oka, T., Remue, E., Meerschaert, K., Vanloo, B., Boucherie, C., Gfeller, D., Bader, G.D., Sidhu, S.S., Vandekerckhove, J., Gettemans, J., and Sudol, M. (2010). Functional complexes between YAP2 and ZO-2 are PDZ domain-dependent, and regulate YAP2 nuclear localization and signalling. Biochem. J. *432*, 461–472.

Pan, D. (2010). The hippo signaling pathway in development and cancer. Dev. Cell *19*, 491–505.

Pradhan, S., Chin, H.G., Estève, P.O., and Jacobsen, S.E. (2009). SET7/9 mediated methylation of non-histone proteins in mammalian cells. Epigenetics *4*, 383–387.

Purcell, D.J., Jeong, K.W., Bittencourt, D., Gerke, D.S., and Stallcup, M.R. (2011). A distinct mechanism for coactivator versus corepressor function by

histone methyltransferase G9a in transcriptional regulation. J. Biol. Chem. *286*, 41963–41971.

Schlegelmilch, K., Mohseni, M., Kirak, O., Pruszak, J., Rodriguez, J.R., Zhou, D., Kreger, B.T., Vasioukhin, V., Avruch, J., Brummelkamp, T.R., and Camargo, F.D. (2011). Yap1 acts downstream of α-catenin to control epidermal proliferation. Cell *144*, 782–795.

Su, I.H., and Tarakhovsky, A. (2006). Lysine methylation and 'signaling memory'. Curr. Opin. Immunol. *18*, 152–157.

Tao, Y., Neppl, R.L., Huang, Z.P., Chen, J., Tang, R.H., Cao, R., Zhang, Y., Jin, S.W., and Wang, D.Z. (2011). The histone methyltransferase Set7/9 promotes myoblast differentiation and myofibril assembly. J. Cell Biol. *194*, 551–565.

van der Flier, L.G., and Clevers, H. (2009). Stem cells, self-renewal, and differentiation in the intestinal epithelium. Annu. Rev. Physiol. *71*, 241–260.

Wang, H., Cao, R., Xia, L., Erdjument-Bromage, H., Borchers, C., Tempst, P., and Zhang, Y. (2001). Purification and functional characterization of a histone H3-lysine 4-specific methyltransferase. Mol. Cell *8*, 1207–1217.

Xiao, B., Jing, C., Wilson, J.R., Walker, P.A., Vasisht, N., Kelly, G., Howell, S., Taylor, I.A., Blackburn, G.M., and Gamblin, S.J. (2003). Structure and catalytic mechanism of the human histone methyltransferase SET7/9. Nature *421*, 652–656.

Yang, X.D., Huang, B., Li, M., Lamb, A., Kelleher, N.L., and Chen, L.F. (2009). Negative regulation of NF-kappaB action by Set9-mediated lysine methylation of the RelA subunit. EMBO J. *28*, 1055–1066.

Yang, J., Huang, J., Dasgupta, M., Sears, N., Miyagi, M., Wang, B., Chance, M.R., Chen, X., Du, Y., Wang, Y., et al. (2010a). Reversible methylation of promoter-bound STAT3 by histone-modifying enzymes. Proc. Natl. Acad. Sci. USA *107*, 21499–21504.

Yang, X.D., Tajkhorshid, E., and Chen, L.F. (2010b). Functional interplay between acetylation and methylation of the RelA subunit of NF-kappaB. Mol. Cell. Biol. *30*, 2170–2180.

Zaph, C., Troy, A.E., Taylor, B.C., Berman-Booty, L.D., Guild, K.J., Du, Y., Yost, E.A., Gruber, A.D., May, M.J., Greten, F.R., et al. (2007). Epithelial-cell-intrinsic IKK-β expression regulates intestinal immune homeostasis. Nature *446*, 552–556.

Zhao, B., Wei, X., Li, W., Udan, R.S., Yang, Q., Kim, J., Xie, J., Ikenoue, T., Yu, J., Li, L., et al. (2007). Inactivation of YAP oncoprotein by the Hippo pathway is involved in cell contact inhibition and tissue growth control. Genes Dev. *21*, 2747–2761.

Zhao, B., Ye, X., Yu, J., Li, L., Li, W., Li, S., Yu, J., Lin, J.D., Wang, C.Y., Chinnaiyan, A.M., et al. (2008). TEAD mediates YAP-dependent gene induction and growth control. Genes Dev. *22*, 1962–1971.

Zhao, B., Li, L., Tumaneng, K., Wang, C.Y., and Guan, K.L. (2010). A coordinated phosphorylation by Lats and CK1 regulates YAP stability through $SCF^{(\beta\text{-}TRCP)}$. Genes Dev. *24*, 72–85.

Zhou, D., Zhang, Y., Wu, H., Barry, E., Yin, Y., Lawrence, E., Dawson, D., Willis, J.E., Markowitz, S.D., Camargo, F.D., and Avruch, J. (2011). Mst1 and Mst2 protein kinases restrain intestinal stem cell proliferation and colonic tumorigenesis by inhibition of Yes-associated protein (Yap) overabundance. Proc. Natl. Acad. Sci. USA *108*, E1312–E1320.

Disease Models & Mechanisms 6, 905-914 (2013) doi:10.1242/dmm.011981

The expanding role of fish models in understanding non-alcoholic fatty liver disease

Yoichi Asaoka[1], Shuji Terai[2], Isao Sakaida[2] and Hiroshi Nishina[1,*]

Non-alcoholic fatty liver disease (NAFLD) is a condition in which excessive fat accumulates in the liver of an individual who has not consumed excessive alcohol. Non-alcoholic steatohepatitis (NASH), a severe form of NAFLD, can progress to hepatic cirrhosis and/or hepatocellular carcinoma (HCC). NAFLD is considered to be a hepatic manifestation of metabolic syndrome, and its incidence has risen worldwide in lockstep with the increased global prevalence of obesity. Over the last decade, rodent studies have yielded an impressive list of molecules associated with NAFLD and NASH pathogenesis. However, the identification of currently unknown metabolic factors using mammalian model organisms is inefficient and expensive compared with studies using fish models such as zebrafish (*Danio rerio*) and medaka (*Oryzias latipes*). Substantial advances in unraveling the molecular pathogenesis of NAFLD have recently been achieved through unbiased forward genetic screens using small fish models. Furthermore, these easily manipulated organisms have been used to great advantage to evaluate the therapeutic effectiveness of various chemical compounds for the treatment of NAFLD. In this Review, we summarize aspects of NAFLD (specifically focusing on NASH) pathogenesis that have been previously revealed by rodent models, and discuss how small fish are increasingly being used to uncover factors that contribute to normal hepatic lipid metabolism. We describe the various types of fish models in use for this purpose, including those generated by mutation, transgenesis, or dietary or chemical treatment, and contrast them with rodent models. The use of small fish in identifying novel potential therapeutic agents for the treatment of NAFLD and NASH is also addressed.

Introduction

Over the past two decades, obesity has become a major public health challenge worldwide. It is clear that as-yet-unrecognized factors governing energy homeostasis must be uncovered in order to protect against the onslaught of metabolic diseases associated with excess adiposity (Dixon, 2010). In fact, the benefits gained from current therapies targeting obesity-related diseases (e.g. hypertension, coronary heart disease, hyperlipidemia and type 2 diabetes) are in danger of being outweighed by the negative effects of increased adiposity (Stewart et al., 2009). Thus, it is urgently necessary to develop systematic and comprehensive approaches to facilitate the identification of factors that play crucial roles in regulating energy homeostasis.

Among the obesity-related diseases, non-alcoholic fatty liver disease (NAFLD; see Box 1 for a full list of abbreviations) has garnered much attention from a broad range of researchers during the last decade. NAFLD is defined as the accumulation of fat in liver cells, known as fatty liver or hepatic steatosis, in the absence of excessive alcohol consumption. According to the practice guidelines of the American Association for the Study of Liver Diseases (AASLD), NAFLD is histologically subdivided into either non-progressive simple steatosis or a more severe condition called non-alcoholic steatohepatitis (NASH). NASH is a progressive chronic liver disease that is initially characterized by inflammation, fibrosis, and degenerative 'ballooning' of hepatocytes (Chalasani et al., 2012). NASH can eventually develop into life-threatening hepatic cirrhosis and/or hepatocellular carcinoma (HCC) after several decades. Indeed, the increased incidence of HCC in individuals with type 2 diabetes is most likely due to the high prevalence of NASH in this population (Ekstedt et al., 2006).

At present, our ability to treat NAFLD, particularly NASH, is constrained by our limited knowledge of the mechanisms underlying the progression of steatosis to more advanced liver inflammation and fibrosis. Researchers have therefore turned to studies of animal models of NAFLD, which are essential tools for gaining a full understanding of the pathophysiology of the human disease. Traditionally, rodent models have been used, and have not only proved helpful for revealing mechanisms underlying human NAFLD or NASH etiology but have also served as important platforms for testing the therapeutic potency of candidate agents (Nagarajan et al., 2012). However, although rodent models have greatly contributed to our understanding of human NAFLD, these results have come at a relatively high financial cost because these animals require considerable staff support and specialized infrastructure. These considerations have spurred the development

[1]Department of Developmental and Regenerative Biology, Medical Research Institute, Tokyo Medical and Dental University, 1-5-45 Yushima, Bunkyo-ku, Tokyo 113-8510, Japan
[2]Department of Gastroenterology and Hepatology, Yamaguchi University Graduate School of Medicine, Minami Kogushi 1-1-1, Ube, Yamaguchi 755-8505, Japan
*Author for correspondence (nishina.dbio@mri.tmd.ac.jp)

Box 1. Abbreviations

AASLD: American Association for the Study of Liver Diseases
Abcb7: ATP-binding cassette sub-family B member 7
ACC1: acetyl CoA carboxylase 1
ACO1: acyl-CoA oxidase 1
Ahcy: S-adenosylhomocysteine hydrolase
Apo: apolipoprotein
CB1R: cannabinoid receptor 1
C/EBP: CCAAT/enhancer-binding protein
Cdipt: CDP-diacylglycerol-inositol 3-phosphatidyltransferase
CHOP-10: C/EBP homologous protein 10
ChREBP: carbohydrate response element-binding protein
CPT1: carnitine palmitoyltransferase 1
DIO: diet-induced obesity
DNL: *de novo* lipogenesis
D-PAS: diastase-periodic-acid-Schiff
EPA: eicosapentaenoic acid
ER: endoplasmic reticulum
FAS: fatty acid synthase
FFA: free fatty acid
HBx: hepatitis B virus X protein
HCC: hepatocellular carcinoma
HCP: hepatitis C virus core protein
HFD: high-fat diet
IL: interleukin
MC4R: melanocortin-4 receptor
NAFLD: non-alcoholic fatty liver disease
NAS: NASH activity score
NASH: non-alcoholic steatohepatitis
NR1H3: nuclear receptor subfamily 1 group H member 3
OHdG: 8-hydroxydeoxyguanosine
PPAR: peroxisome proliferator-activated receptor
PUFA: polyunsaturated fatty acid
ROS: reactive oxygen species
SIRT1: sirtuin-1
SREBP: sterol regulatory element-binding protein
TAA: thioacetamide
TALEN: transcription activator-like effector nuclease
Tel: telmisartan
TILLING: targeting induced local lesions in genomes
TNF: tumor necrosis factor
TRAPPC11: trafficking protein particle complex 11
UPR: unfolded protein response
VLDL: very low-density lipoprotein
WT: wild-type
YY1: yin yang 1
ZFN: zinc finger nuclease

of simpler and less expensive animal models to complement rodent-based research. Recent reports on energy homeostasis in worms, flies and small fish have shown that lower organisms can be used to accurately unravel metabolic processes underlying obesity in mammals (Schlegel and Stainier, 2007). Being vertebrates, small fish are structurally much more similar to humans than are worms and flies, and so have been exploited to successfully model various human diseases (Goldsmith and Jobin, 2012). In this Review, we discuss our current understanding of NAFLD (particularly NASH) pathogenesis as deduced from work with several fish models of this disease. We anticipate that insights emerging from these models will ultimately translate into the development of novel therapeutics for the treatment of severe human NAFLD.

NASH pathogenesis: a 'two-hit' model

The pathogenesis of NASH is thought to involve a two-step process in which the first 'hit' is excessive triglyceride accumulation in the liver that leads to NAFLD (Fig. 1A). The second 'hit', which results in NASH, is thought to involve additional pathogenic factors that can eventually induce liver damage, such as inflammatory cytokines, oxidative stress, mitochondrial dysfunction and/or endoplasmic reticulum (ER) stress (Day and James, 1998).

The first 'hit'

As summarized above, the initial step (NAFLD development) involves the hepatic accumulation of triglycerides. Triglycerides are produced by the esterification of free fatty acids (FFAs) and glycerol within hepatocytes (Fig. 1B). FFAs are derived from three distinct sources: (1) circulating fatty acids released from adipose tissue, (2) dietary sources, and (3) *de novo* lipogenesis (DNL) (Postic and Girard, 2008). FFAs can be metabolized by one of two pathways: β-oxidation to generate ATP, or esterification to produce triglycerides. These triglycerides are either stored in lipid droplets within hepatocytes, or are packaged and released as very low-density lipoprotein (VLDL) particles into the blood. In the fasting state, the contribution of DNL to the hepatic triglyceride pool is normally quite low. However, DNL is highly elevated in hepatocytes of individuals who are insulin-resistant and have NAFLD (Schwarz et al., 2003). This insulin resistance is manifested as hyperinsulinemia and hyperglycemia. In the livers of these individuals, hyperinsulinemia leads to the upregulation of SREBP-1c, the master transcriptional regulator of all lipogenic genes. Simultaneously, hyperglycemia activates carbohydrate-responsive element binding protein (ChREBP), which transcriptionally activates genes that are involved in DNL and thus promotes an imbalance in lipid input relative to output; this imbalance then results in hepatic steatosis (Fig. 1B).

The second 'hit'

The role of inflammatory cytokines and adipokines

The progression of NAFLD to NASH is largely driven by liver Kupffer cells, which secrete a variety of inflammatory cytokines. TNFα production is one of the earliest events in liver injury and triggers the secretion of other cytokines that recruit inflammatory cells, kill hepatocytes and initiate fibrogenesis. In rodent studies, TNFα was shown to be dysfunctionally released when animals exhibited hepatic steatosis, and this TNFα contributed to NASH severity (Diehl, 2002). Hepatic levels of TNFα are consistently elevated in humans with NASH and again correlate with histological severity. Furthermore, emerging evidence suggests that inflammation in any tissue can promote carcinogenesis, and that the chronic inflammatory state associated with hepatic steatosis might play a crucial role in HCC progression (Day, 2006).

In addition to cytokines released by the liver, cytokines synthesized by adipose tissues can contribute to NASH. Adipokines are a subset of adipose-tissue-derived cytokines whose functional roles in NAFLD have recently been recognized. For example, leptin is an adipokine secreted mainly by mature adipocytes. The functions of leptin include the regulation of energy intake and consumption, modulation of the immune system, and induction of inflammatory and fibrogenic signals. Elevated leptin levels are frequently observed in individuals with NAFLD, which is now

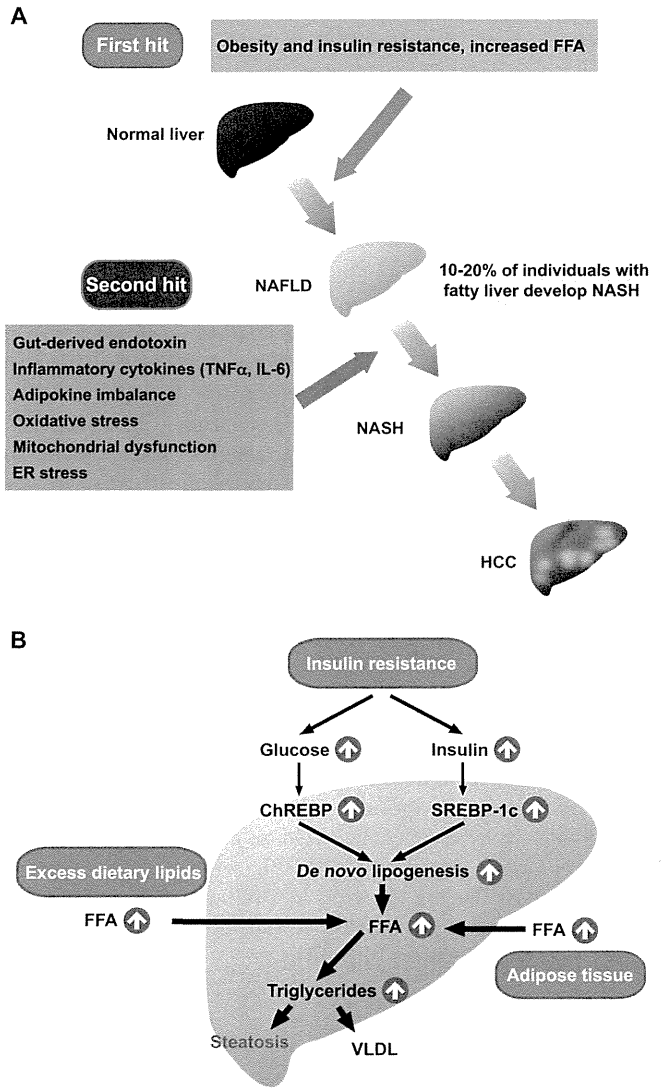

Fig. 1. Mechanisms of NASH: the two-hit model. (A) In the two-hit hypothesis of liver disease development, steatosis (fatty liver causing NAFLD) represents the 'first hit' that sensitizes the liver to injury mediated by 'second hits', such as from endotoxin, inflammatory cytokines, adipokines, oxidative stress, mitochondrial dysfunction and/or ER stress. Receipt of both hits leads to the steatohepatitis and fibrosis of NASH, and eventually the development of hepatocellular carcinoma. (B) Obesity and insulin resistance lead to an increased release of FFA from adipose tissues and enhanced FFA flux to the liver. In the liver, hyperinsulinemia induces SREBP-1c expression, which increases *de novo* lipogenesis via activation of lipogenic gene transcription. At the same time, hyperglycemia activates ChREBP, which also activates the transcription of lipogenic genes, increasing *de novo* lipogenesis and FFA levels. These fatty acids can either be oxidized in the mitochondria to generate ATP, or esterified to produce triglycerides. These triglycerides are either incorporated into VLDL for export from hepatocytes, or are stored within hepatocytes, leading to steatosis.

deemed to be a leptin-resistant condition (Huang et al., 2008). Some researchers therefore believe that leptin plays a key role in NAFLD development.

Adiponectin is another well-studied adipokine that exerts anti-inflammatory effects and increases insulin sensitivity. The secretion and circulating levels of adiponectin are inversely correlated with body fat content and are decreased in individuals with NAFLD (Bugianesi et al., 2005). In murine models of NAFLD, administration of adiponectin suppresses liver enlargement and improves the biochemical and histological signs of NAFLD (Tomita et al., 2008; Xu et al., 2003). Furthermore, adiponectin attenuates the effects of TNFα, which reciprocally suppresses adiponectin production (Whitehead et al., 2006). The importance of adiponectin in NAFLD is supported by studies indicating that serum adiponectin levels can help to predict the severity of liver injury in individuals with NAFLD (Lemoine et al., 2009).

Oxidative stress and mitochondrial dysfunction

Recent studies have revealed the important roles of oxidative stress and subsequent mitochondrial dysfunction in NAFLD and NASH, with the stage and grade of NAFLD correlating with the level of oxidative stress (Chalasani et al., 2004). Normally, fatty-acid β-oxidation within the liver occurs in the mitochondria. However, in the context of NAFLD, this process can become impaired as a result of the increased FFA load, leading to the generation of reactive oxygen species (ROS) (Sanyal et al., 2001). ROS can cause oxidative stress, which in turn upregulates inflammatory pathways and causes mitochondrial damage. Structural mitochondrial abnormalities (enlarged mitochondria, loss of mitochondrial cristae and presence of paracrystalline inclusion bodies) and impaired mitochondrial electron transport chain enzyme activity have been observed in humans with NASH (Pessayre and Fromenty, 2005).

ER stress

ER stress is another pathogenic mechanism implicated in NASH development (Day, 2006). The ER is one of the largest cellular organelles and serves many specialized functions, including the translocation of secretory proteins across the ER membrane, insertion of membrane proteins, protein folding and modification in the ER lumen, phospholipid biosynthesis, and detoxification. The disruption of ER homeostasis constitutes ER stress, which can be induced by a variety of biological insults such as hyperinsulinemia and hyperlipidemia. ER stress can subsequently upregulate various signaling pathways, leading to insulin resistance, inflammation, mitochondrial dysfunction and apoptosis (Day, 2006). The involvement of ER stress in NAFLD is less well studied than in obesity, diabetes and cardiovascular disease, despite evidence that it plays a part in NAFLD pathogenesis (Puri et al., 2008).

Fish models of NAFLD and NASH

Advantages of fish models

As noted above, rodents are the traditional organisms used to uncover mechanisms underlying diseases of the liver, as well as to establish diagnostic criteria and medical therapies for individuals with liver disease. For example, melanocortin-4-receptor-deficient (MC4R-KO) mice can be induced to develop a liver condition that is similar to human NASH (Itoh et al., 2011). MC4R is a seven-transmembrane G-protein-coupled receptor that is expressed by cells in the hypothalamus and is involved in the control of feeding behavior and body weight (Balthasar et al., 2005). After 20 weeks of feeding on a high-fat diet (HFD), MC4R-KO mice exhibit obesity, insulin resistance and dyslipidemia.

These mutants then develop multiple HCCs if maintained on the HFD for another 7 months. Thus, this strain has been used to investigate the sequence of events leading to hepatic steatosis, liver fibrosis and HCC (Itoh et al., 2011). However, like all rodent models, the use of the MC4R-KO mouse is hampered by certain limitations that do not apply to fish models of this disease. Rodent models are not necessarily suited to large-scale drug screening because these animals have a relatively large body size, produce small litters and incur high husbandry costs. Furthermore, to examine their livers for abnormalities, rodents must be sacrificed and their internal organs surgically isolated. This requirement does not allow for parallel, continuous, real-time monitoring of liver condition in multiple animals.

Small fish such as zebrafish (*Danio rerio*) and medaka (*Oryzias latipes*) have a short generation time, are highly fertile, and cost little in terms of housing space and daily maintenance owing to their tiny size. They are also much easier to screen for abnormal phenotypes because their larvae are optically clear and their internal organs can be directly observed without the need for surgery. Thus, real-time, simultaneous monitoring of livers in multiple animals is easily achieved. Zebrafish and medaka have therefore been increasingly used as alternatives to rodents for vertebrate developmental and toxicological studies, as well as for drug screening and evaluation programs. In addition, lipids can be visualized directly in live zebrafish using fluorescent fatty-acid analogs (Carten et al., 2011), making these small fish powerful models for studying lipid-related diseases such as NAFLD. We and other groups have successfully elucidated various aspects of NAFLD and NASH induction by using zebrafish and medaka that have naturally occurring or engineered mutations of certain genes, or express engineered transgenes. Alternatively, these fish have been subjected to HFD feeding or treatment with a carcinogenic chemical compound to induce NAFLD or NASH. In the following sections, we review the results of research that has made use of these approaches.

Mutant fish models of NAFLD and NASH

At present, several fish mutants with hepatic steatosis have been characterized. The affected genes and phenotypes of these animals are summarized in Table 1.

foie gras (*fgr*) zebrafish

The *foie gras* (*fgr*) zebrafish mutant was the first fish to be reported as a model of hepatic steatosis (Sadler et al., 2005). This mutant was identified in a screen for hepatomegaly at day 5 of embryogenesis. The livers of *fgr* mutants exhibit enlarged hepatocytes, hepatocyte nuclear degeneration and steatosis. Thus, *fgr* fish display most of the hallmarks of mammalian NASH, with the exception of inflammation. These *fgr* defects can be phenocopied by a translation-blocking morpholino, suggesting that *fgr* is a null mutation. The Fgr protein is the zebrafish ortholog of human TRAPPC11 (trafficking protein particle complex 11), which is involved in ER-to-Golgi trafficking (Scrivens et al., 2011). Interestingly, Cinaroglu et al. found that the *fgr* mutation causes hepatic ER stress that is linked to hepatic steatosis (Cinaroglu et al., 2011). Furthermore, this ER stress causes hepatocyte apoptosis that is controlled in part through the *atf6* gene, which is involved in the unfolded protein response (UPR). Morpholino blockade of *atf6* can prevent the liver injury that occurs in *fgr* mutants experiencing chronic ER stress. However, *atf6* blockade potentiates the steatosis that develops in wild-type (WT) zebrafish when acute ER stress is induced by treatment with the toxin tunicamycin (Cinaroglu et al., 2011). These results suggest that Atf6 might have different effects in acute and chronic phases of liver injury.

namako (*nmk*) medaka

A screen designed to isolate medaka mutants with abnormal livers identified the *namako* (*nmk*) mutant (Miyake et al., 2008). The liver in *nmk* medaka develops normally until hatching but, by 2 days post-hatching, this organ exhibits altered morphology and loss of transparency. The mutant hepatocytes are arranged in a random

Table 1. List of mutant fish models of liver disease

Species	Mutant	Gene	Function	Liver phenotypes	Knockout mice	Reference
Zebrafish	*foie gras*	*Trafficking protein particle complex 11 (trappc11)*	ER-to-Golgi trafficking	Hepatic steatosis; nuclear degeneration of hepatocytes	Not characterized yet	Sadler et al., 2005
Medaka	*nmk*	*ATP-binding cassette sub-family B member 7 (abcb7)*	Lipid and iron metabolism	Hepatic steatosis	Knockout mice die early in gestation	Miyake et al., 2008
Zebrafish	*ducttrip*	*S-adenosyl-homocysteine hydrolase (ahcy)*	Methionine metabolism	Hepatic steatosis; mitochondrial dysfunction; liver degeneration	Not characterized yet	Matthews et al., 2009
Zebrafish	*hi559*	*CDP-diacylglycerol-inositol 3-phosphatidyltransferase (cdipt)*	Phospholipid synthesis	Hepatic steatosis	Not characterized yet	Thakur et al., 2011
Zebrafish	*hu1960, hu1968*	*Serine/threonine kinase 11 (stk11)*	Phosphorylation of the nutritional sensor AMP-kinase	Fasting hepatic steatosis; glycogen depletion	Homozygous deletion mutants die at midgestation	van der Velden et al., 2011
Zebrafish	*red moon*	*Solute carrier family 16a member 6a (slc16a6a)*	β-hydroxybutyrate transporter	Fasting hepatic steatosis	Not characterized yet	Hugo et al., 2012
Zebrafish	*st67*	*Sec63*	ER translocon machinery	Disrupted bile canaliculi; accumulation of large lysosomes; hepatic steatosis	Tissue-specific homozygous mutations result in kidney and liver cyst formation	Monk et al., 2013

manner and vacuoles are plentiful, evoking the pathology of rodent hepatic steatosis. Furthermore, the mitochondria in *nmk* livers tend to be enlarged and swollen, a characteristic of fatty liver. Positional cloning of the gene responsible for the *nmk* phenotype revealed that a mutation in the ATP-binding cassette sub-family B member 7 gene (*abcb7*) causes an Asp substitution at the Val residue in position 219, which is an amino acid conserved among most vertebrate species. The expression of genes involved in iron and lipid metabolism is also affected in *nmk* liver. Among these genes, *apoliporotein* (*apo*) *B-100* and *apoE* are thought to play important roles in the pathogenesis of fatty liver. These proteins are both components of VLDL and positively control its production rate. Thus, ApoB-100 and ApoE are rate-determining factors in hepatocyte-lipid export. In line with this, *apoE* deficiency in mice leads to hepatic steatosis (Mensenkamp et al., 2000).

ducttrip (*dtp*) zebrafish

The *ducttrip* (*dtp*) zebrafish mutant was originally isolated in a chemical mutagenesis screen for defects in exocrine pancreas development (Yee et al., 2005). Subsequent experiments revealed that the *dpt* mutant displays hepatic steatosis, mitochondrial dysfunction and liver degeneration (Matthews et al., 2009). Positional cloning identified a causative mutation in the *ahcy* gene, which encodes S-adenosylhomocysteine hydrolase. This enzyme is crucial for the hydrolysis of S-adenosylhomocysteine to homocysteine and adenosine, a pathway whose disruption has been linked to mitochondrial dysfunction and hepatic steatosis. The *dtp* mutant shows elevated expression of *TNFα* and *PPARγ* genes, which is thought to occur via an epigenetic mechanism involving changes in histone methylation coding (Matthews et al., 2009). Such changes can trigger an inflammatory reaction marked by enhanced TNFα production.

hi559 zebrafish

The signaling pathways that maintain hepatic homeostasis are highly conserved, as demonstrated by studies of the *hi559* zebrafish mutant. The *hi559* mutant has an inactivating insertion in the *CDP-diacylglycerol-inositol 3-phosphatidyltransferase* (*cdipt*) gene (Thakur et al., 2011). This mutation eliminates phosphatidyl inositol synthesis, and the lack of this crucial phospholipid in the liver seems to induce persistent hepatocyte ER stress marked by activation of the UPR. Concurrent with the presence of ER stress, the *hi559* liver displays NAFLD pathologies, including macrovesicular steatosis, hepatocyte ballooning and necroapoptosis. Subsequent analysis of the ultrastructural pathology of *hi559* hepatocytes has demonstrated that the morphology of their mitochondria is abnormal, although it is unknown whether this structural change affects fatty-acid β-oxidation (Thakur et al., 2011). The *hi559* mutant was the first *in vivo* model linking phosphatidyl inositol synthesis, ER stress and NAFLD. As such, this finding confirms that additional work investigating the requirement for phosphatidyl inositol in molecular pathways of normal hepatic lipid metabolism is merited.

Transgenic fish models

Several research groups have attempted to create NAFLD and NASH models in small fish using transgenic approaches (Table 2).

HBx zebrafish

Shieh et al. demonstrated that engineered expression of the hepatitis B virus X protein (HBx) in zebrafish induces hepatic steatosis by upregulating C/EBP-α, SREBP1 and ChREBP, three important adipogenic genes that drive *de novo* FFA synthesis (Shieh et al., 2010). Histological examination of the livers of multiple independent HBx transgenic lines showed that they all exhibited hepatic steatosis, lobular inflammation and hepatocyte ballooning. This study was the first report demonstrating that forced expression of HBx *in vivo* can cause a wide range of liver disease phenotypes in lower vertebrates.

Gankyrin, YY1 and CB1R zebrafish

Three transgenic zebrafish models of hepatic steatosis have been generated by the group of Her (National Taiwan Ocean University). In the first of these models, hepatic lipid accumulation was studied

Table 2. List of transgenic fish models of liver disease

Species	Transgenic line	Transgene	Liver phenotypes	Reference
Zebrafish	*Tg(–2.8fabp10a:HBV.HBx-GFP)*	Hepatitis B virus *X protein* (*HBx*)	Hepatic steatosis; lobular inflammation; balloon degeneration (similar to NASH)	Shieh et al., 2010
Zebrafish	*Tg(–2.8fabp10a:EGFP-psmd10)*	*proteasome 26S subunit, non-ATPase, 10* (*gankyrin*)	Hepatic steatosis	Her et al., 2011
Zebrafish	*Tg(fabp10:EGFP-krasV12)*	$kras^{V12}$	Liver hyperplasia; hepatocellular carcinoma	Nguyen et al., 2011; Nguyen et al., 2012
Zebrafish	*Tg(fabp10:TA; TRE:xmrk; krt4:GFP)*	*Xiphophorus melanoma receptor kinase* (*xmrk*)	Hepatocellular carcinoma	Li et al., 2012
Medaka	*Tamoxifen-inducible medaka myc17 transgenic line*	*medaka myc17*	Liver hyperplasia	Menescal et al., 2012
Zebrafish	*Tg(lfabp:dnfgfr1-egfp)*	*dominant-negative fibroblast growth factor receptor 1* (*dnfgfr1*)	Hepatic steatosis	Tsai et al., 2013
Zebrafish	*Tg(–2.8fabp10a:gfp-YY1)*	*yin yang 1* (*yy1*)	Hepatic steatosis	Her et al., 2013
Zebrafish	*Tg(–2.8fabp10a:Tetoff-CB1R:2A:eGFP)*	*cannabinoid receptor 1* (*cb1r*)	Hepatic steatosis	Pai et al., 2013
Zebrafish	*Tg(fabp10:TA; TRE:Myc; krt4:GFP)*	*mouse myc*	Liver hyperplasia; hepatocellular adenoma and carcinoma	Li et al., 2013

in *gankyrin* transgenic zebrafish (Her et al., 2011). Gankyrin is a small ankyrin-repeat protein previously shown to be involved in normal cellular proliferation as well as in HCC tumorigenesis (Higashitsuji et al., 2000). Over 90% of viable adult *gankyrin* transgenic zebrafish exhibit an increase in hepatic lipid content that leads to liver steatosis. Molecular analysis revealed that *gankyrin* overexpression induces hepatic steatosis and modulates the expression profiles of four hepatic microRNAs involved in lipid metabolism. This study was the first to demonstrate that *gankyrin* overexpression is pathological and induces the development of liver steatosis via dysregulation of hepatic microRNAs. In the two other transgenic zebrafish models described by Her's group, hepatic steatosis is induced by liver-specific overexpression of yin yang 1 (YY1) or by cannabinoid receptor 1 (CB1R) (Her et al., 2013; Pai et al., 2013). YY1 induces the expression of important lipogenic genes, such as *C/EBP-α*, *PPARγ* and *SREBP-1c*, by inhibiting C/EBP homologous protein 10 (CHOP-10) expression, whereas CB1R stimulates the expression of *SREBP-1c*. In turn, the upregulation of those lipogenic factors drives DNL, which is expected to lead to hepatic accumulation of FFA and triglycerides.

Lfabp:dnfgfr1-egfp zebrafish

Another transgenic zebrafish that is used to study hepatic steatosis was generated by expressing a dominant-negative Fgf receptor mutation specifically in hepatocytes (*lfabp:dnfgfr1-egfp*) (Tsai et al., 2013). Hepatocytes in young *lfabp:dnfgfr1-egfp* zebrafish display hepatocyte ballooning, whereas adult fish display hepatic steatosis and cholestasis. These findings confirm that liver homeostasis is dysregulated when Fgf signaling is repressed. This analysis closely paralleled the mouse studies of Steiling et al., which demonstrated that hepatocellular expression of dominant-negative FGFR2b accelerates the development of fatty liver in aged transgenic animals (Steiling et al., 2003). This similarity of results achieved in mouse and fish models reinforces the validity of exploiting the latter to study NAFLD. In particular, the genetic tractability of fish and the ability to examine the entire pathological process *in vivo* are particular strengths of small fish models of hepatic steatosis.

Dietary fish models

HFD-medaka

Our group has developed a NASH model in medaka that is based on feeding the fish a HFD (Matsumoto et al., 2010) (Table 3). Medaka that consume a HFD (HFD-medaka) exhibit hyperlipidemia, hyperglycemia and the hepatocyte ballooning that is a key diagnostic feature of human NASH (Brunt et al., 1999; Matteoni et al., 1999; Neuschwander-Tetri and Caldwell, 2003). The frequency of ballooning in WT medaka is 10-20% (Boorman et al., 1997; Brown-Peterson et al., 1999; Bunton, 1990), whereas over 60% of HFD-medaka exhibited this phenotype. In contrast, it was reported that only 46% of C57BL/6 mice fed a HFD develop steatohepatitis (Deng et al., 2005). Therefore, the medaka model of NASH is slightly superior to the rodent model (64% vs 46% efficiency) in terms of inducing the ballooning degeneration of hepatocytes typical of this disease.

Hepatocytes of HFD-medaka show increased expression of lipogenic genes (*SREBP-1c*, *FAS* and *ACC1*) and decreased expression of lipolytic genes (*PPARα* and *CPT1*). These data suggest that HFD-medaka suffer from increased fatty-acid synthesis accompanied by decreased fatty-acid β-oxidation and inflammation, accounting for their fatty livers. Previously, it was reported that treatment with n-3 polyunsaturated fatty acid (PUFA), a mixture of eicosapentaenoic acid (EPA) and docosahexaenoic acid, improves features of hepatic steatosis and necroinflammation in humans (Capanni et al., 2006). The EPA-evoked anti-inflammatory effects are thought to result from mechanisms involving decreased FFA-derived lipotoxicity in liver cells (Sekiya et al., 2003), and administration of EPA has been investigated as a therapy for human NASH (Tanaka et al., 2008). In light of these findings, we explored whether EPA treatment could suppress disease progression in our medaka NASH model. Treatment of HFD-medaka with EPA alleviates the disease phenotypes, as judged by the recovery of normal liver fatty-acid composition and normal expression levels of lipogenic and lipolytic genes. In addition, medaka fed an n-3 PUFA-deficient diet develop NASH features. Thus, NASH can be induced in medaka by a HFD, and the proportion of n-3 PUFAs in the liver affects NASH pathogenesis in these fish. Subsequent work has confirmed that this medaka NASH model is helpful for advancing our understanding of human NASH pathology and can assist in the clinical development of novel therapeutics, as described below (Kuwashiro et al., 2011; Oishi et al., 2012).

DIO-zebrafish

Oka et al. have used an alternative dietary approach to establish a zebrafish model of diet-induced obesity (DIO) with NAFLD features

Table 3. List of dietary- or chemical-treated fish models of liver disease

Species	Animal model	Liver phenotypes	Reference
Medaka	Diethylnitrosamine-treated fish	Hepatomas	Ishikawa et al., 1975
Medaka	Methylazoxymethanol-acetate-treated fish	Hepatic tumors	Aoki and Matsudaira, 1977
Zebrafish	γ-hexachlorocyclohexane-treated fish	Hepatic steatosis	Braunbeck et al., 1990
Zebrafish	Thioacetamide-treated fish	Steatohepatitis	Amali et al., 2006
Zebrafish	Thioacetamide-treated HCP transgenic fish	Steatohepatitis; cirrhosis; HCC	Rekha et al., 2008
Zebrafish	EtOH-treated fish	Alcoholic liver disease	Passeri et al., 2009; Howarth et al., 2012
Zebrafish	HFD-fed fish	Hepatic steatosis	Oka et al., 2010; Tainaka et al., 2011
Medaka	HFD-fed fish	NASH	Matsumoto et al., 2010; Kuwashiro et al., 2011; Oishi et al., 2012
Zebrafish	Aflatoxin-B1-treated HBx transgenic fish	Hepatic steatosis; hepatitis; liver hyperplasia	Lu et al., 2013

(Oka et al., 2010). Zebrafish overfed with *Artemia* (DIO-zebrafish) exhibit increased body mass index, hypertriglyceridemia and hepatic steatosis. Comparative transcriptome analysis of visceral adipose tissue revealed that the pathophysiological pathways associated with mammalian obesity are similarly altered in DIO-zebrafish. In both DIO-zebrafish and obese mammals, dysregulation of genes involved in the blood coagulation pathway, such as *apoH*, *interleukin-6* (*IL-6*) and *IL-1β*, and genes involved in lipid metabolism, such as *SREBP1*, *PPARα/γ*, *NR1H3* and *leptin*, has been observed. These findings suggest that DIO-zebrafish, like HFD-medaka, could be useful for identifying putative pharmacological targets and testing novel chemical compounds for the treatment of human hepatic steatosis (Fig. 2).

Chemically treated fish models

In Japan, the history of medaka as a research organism began in the 1970s with the investigation of their use as a liver tumor model. Indeed, medaka proved to be an organism that is sensitive to many carcinogens and is thus highly useful for tumorigenesis research (Aoki and Matsudaira, 1977; Ishikawa et al., 1975). Starting in the 1990s, models of hepatic steatosis were established in zebrafish by treating them with a potent hepatotoxic agent such as γ-hexachlorocyclohexane or thioacetamide (TAA) (Table 3) (Amali et al., 2006; Braunbeck et al., 1990). Subsequently, Rekha et al. reported that zebrafish that overexpress hepatitis C virus core protein (HCP) and are treated with TAA develop HCCs faster than standard mouse models (Rekha et al., 2008). The speed of this particular zebrafish HCC model could make it a powerful platform for screening for drugs that are effective against HCCs.

Screening for drugs relevant to NAFLD

In addition to advancing basic research into NAFLD mechanisms, small fish have proved useful in novel assay systems designed to screen for new candidate drugs for these disorders (Fig. 2A). Several pharmaceutical companies have developed drug discovery methodologies based on high-throughput *in vivo* drug screening using small fish models of human diseases. The HFD-medaka NASH model (Matsumoto et al., 2010) has been particularly helpful for the investigation of candidate drug effectiveness (Table 4), owing to its similarity to human NAFLD (particularly NASH).

Insights into drug efficacy from the HFD-medaka model

In 2011, our group published a study in which we used our HFD-medaka NASH model to investigate the efficacy of the anti-hypertensive drug telmisartan (Tel) (Kuwashiro et al., 2011). This drug blocks angiotensin-II type 1 receptors, excites PPARγ, and reportedly improves glycolipid metabolism in humans. Using the NASH activity score (NAS), a classification system for human NASH pathology in clinical settings (Kleiner et al., 2005), we assessed liver histology in our HFD-medaka NASH model and confirmed that the NAS increases over time in the absence of Tel. Treatment of HFD-medaka with Tel results in an increase in the expression of liver *PPARγ*, *CPT1* and *ACO1*, a decrease in the number of 8-hydroxydeoxyguanosine (OHdG)-positive hepatocytes in livers, and a reduction in the infiltration of macrophages that are positive for diastase-periodic-acid-Schiff (D-PAS). Thus, Tel administration might induce the β-oxidation of FFAs in the liver of HFD-medaka and thereby contribute to the reduction of triglycerides in this organ. Interestingly, the fatty-acid content of the liver in these fish is not affected. These results demonstrate

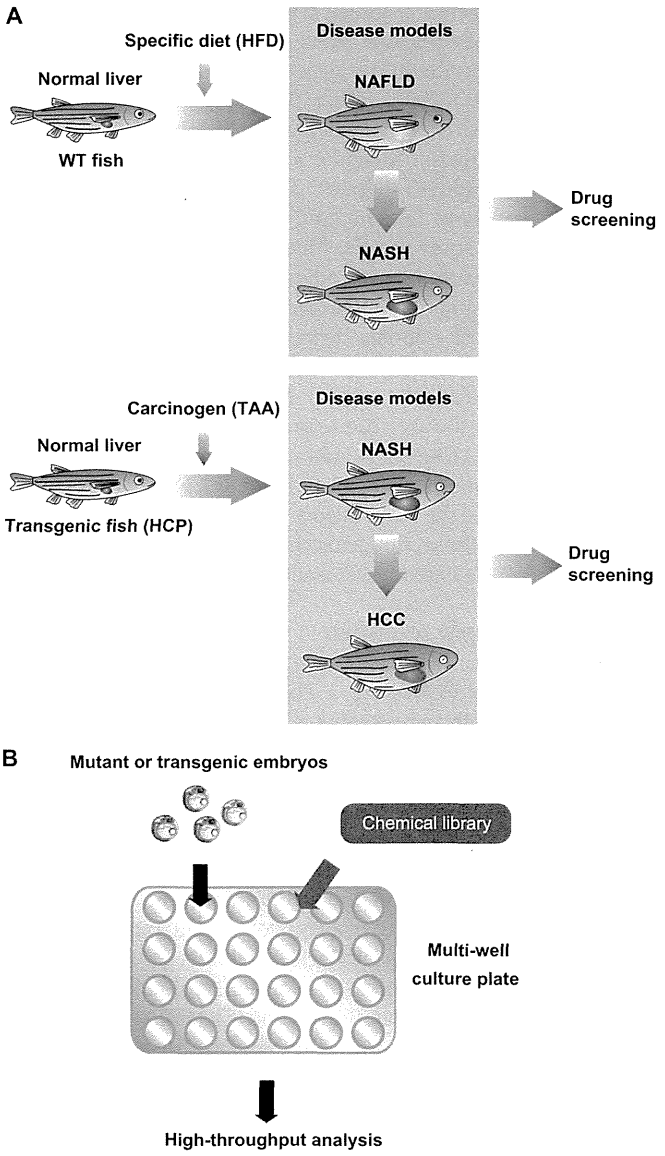

Fig. 2. Drug screening strategy using fish disease models. (A) An overview of the NAFLD, NASH and HCC drug screening strategy in fish models. WT or transgenic (HCP) fish are raised on a specific diet (HFD) or treated with a specific carcinogen (TAA), giving rise to NAFLD and NASH, or NASH and HCC, respectively. The disease models are exposed to candidate drugs to determine whether the development of NAFLD, NASH or HCC can be mitigated. (B) Small-molecule inhibitor screen. Chemical libraries can be aliquoted to multi-well plates that contain fish growth medium. Large numbers of mutant or transgenic fish can be mated to generate thousands of embryos, which are placed in the multi-well plates containing medium and test reagents. These multi-well plates easily allow the detailed observation of embryo morphology under a dissecting microscope. To investigate chemical-induced changes in specific markers, several techniques have been established to perform high-throughput analysis, such as whole-mount immunohistochemistry or whole-mount *in situ* hybridization on large numbers of embryos.

Table 4. List of drugs investigated using fish models of liver disease

Drug	Fish model	Reference
n-3 PUFA	HFD-medaka	Matsumoto et al., 2010
Telmisartan (Tel)	HFD-medaka	Kuwashiro et al., 2011
Ezetimibe	HFD-medaka	Oishi et al., 2012
Campari tomato	DIO-zebrafish	Tainaka et al., 2011
Taurine	TAA-treated zebrafish	Hammes et al., 2012
PK 11195	*Tg(pck1:Luc2)* zebrafish	Gut et al., 2013

that Tel administration can ameliorate NASH pathology in HFD-medaka and improve their NAS values.

We have also examined the effects of ezetimibe in our HFD-medaka NASH model (Oishi et al., 2012). Ezetimibe is a small-molecule inhibitor of the intestinal cholesterol transporter encoded by the Niemann-Pick C1-like 1 (*NPC1L1*) gene and is used to treat individuals with high blood cholesterol levels. We found that ezetimibe treatment of HFD-medaka reduces total cholesterol and triacylglycerol in the blood, as expected. However, ezetimibe also induces a significant decrease in fatty acids in the liver. The expression levels of genes related to hepatic fatty-acid metabolism are also reduced by ezetimibe administration. Histological examination of the livers of ezetimibe-treated HFD-medaka revealed reductions in the number of inflammatory cells and the NAS value. This decrease in liver fatty acids indicates that the NASH symptoms in HFD-medaka can be mitigated by ezetimibe, a finding with potential implications for treatment of the human disease.

Insights into drug efficacy from zebrafish models

Recently, several epidemiological studies have demonstrated that high dietary intake of vegetable products is beneficial against obesity and its related diseases. For example, tomato and its components were shown to lower plasma cholesterol and triacylglyceride and prevent obesity-related diseases, including hypertension in humans (Engelhard et al., 2006) and NASH-promoted hepatocarcinogenesis in rats (Wang et al., 2010). In 2011, Tainaka et al. used DIO-zebrafish to evaluate the influence of certain food components on the development of human hepatic steatosis. Zebrafish are polyphagous animals and readily eat human foods, making them highly suitable for feeding experiments designed to perform *in vivo* screening of orally administered test compounds. In this particular study, DIO-zebrafish were subjected to transcriptomic analysis to test the effects on gene expression of certain vegetables (Tainaka et al., 2011). Among all vegetables tested, Campari tomato suppressed diet-induced obesity in zebrafish, as judged by reductions in dyslipidemia and hepatic steatosis, and the downregulation of lipogenic genes such as *SREBP1*. This is the first study to use zebrafish for food component evaluation, and its results indicate that DIO-zebrafish are a powerful tool for identifying foods that can serve as natural medicines for the prevention or treatment of human hepatic steatosis.

Zebrafish have also been used to test taurine (2-aminoethanesulfonic acid) as a hepatoprotective agent (Hammes et al., 2012). Taurine has been hypothesized to protect against TAA-mediated hepatic steatosis because of its hypolipidemic and antioxidant effects (Balkan et al., 2001). Compared with zebrafish treated with TAA alone, TAA-treated zebrafish that also receive taurine show reductions in liver lipid accumulation and oxidative stress parameters. These findings are in agreement with the rodent model results of Chen et al., which showed that oxidative stress is decreased and histological parameters of hepatic steatosis are improved in NASH-affected rats that are treated with taurine (Chen et al., 2006). Additional examination of taurine+TAA-treated zebrafish has revealed that taurine decreases hepatic steatosis by increasing *sirtuin-1* (*sirt1*) mRNA expression. SIRT1 is a nicotinamide adenine dinucleotide (NAD^+)-dependent deacetylase that has recently been shown to protect against NAFLD pathogenesis (Colak et al., 2011). The study of Hammes et al. is the first to evaluate the effect of taurine on SIRT1 expression in hepatic steatosis (Hammes et al., 2012). On the basis of these results, taurine might be a promising therapy for human NASH.

Gut et al. have recently described an innovative drug discovery strategy in which transgenic reporter zebrafish were used to identify small molecules that can modulate the expression of the fasting-inducible gluconeogenic gene *pck1* (Gut et al., 2013). Transgenic zebrafish expressing a bioluminescence reporter gene under the control of the *pck1* promoter were generated and treated with drugs known to affect gluconeogenesis in humans, as well as with several metabolically uncharacterized compounds. It was found that the translocator protein ligands PK 11195 and Ro5-4864 decrease glucose levels in the reporter fish despite a strong inductive effect on the *pck1* promoter. Notably, when translated to a mammalian system, PK 11195 treatment prevents the hepatic steatosis and glucose intolerance that develop in obese mice fed a HFD (Gut et al., 2013). These results validate the zebrafish data in the mammalian context and help to build a framework that is suitable for developing a new class of drugs for metabolic diseases.

Concluding remarks

Zebrafish and medaka are emerging as powerful model animals for generating novel insights into the mechanisms of NAFLD. Indeed, the analyses of NAFLD pathogenesis in these mutant fish models have identified important biological players, including Trappc11 and Cdipt, that have yet to be examined in mammals. NAFLD fish models and transgenic reporter fish have also been useful for drug testing, with n-3 PUFA, Tel, ezetimibe, taurine, certain vegetables, and translocator protein ligands all proven to be effective in reducing NASH pathology. In fact, some of these drugs, such as n-3 PUFA, have recently been recommended as potential NAFLD and NASH pharmacotherapies under the AASLD guidelines (Chalasani et al., 2012). We anticipate that NAFLD and NASH fish models will soon be utilized for additional therapeutic screening efforts.

The findings summarized in this Review highlight that natural and engineered fish models of NAFLD are useful tools for dissecting the still unknown mechanisms underlying non-alcoholic liver disease in humans. In addition, several new genomics technologies, such as 'targeting induced local lesions in genomes' (TILLING), zinc finger nuclease (ZFN) and transcription activator-like effector nuclease (TALEN), have been developed to perform more rapid targeted gene disruption in zebrafish and medaka (Huang et al., 2012). Together with transgenesis, the Cre-*loxP* system and various other inducible systems available for small fish, these genomic

engineering tools are likely to accelerate the development of fish models of NAFLD that can be exploited to yield additional novel insights into this disease.

COMPETING INTERESTS

The authors declare that they do not have any competing or financial interests.

FUNDING

This work was supported by a Grant-in-Aid for Scientific Research on Innovative Areas from the Ministry of Education, Culture, Sports, Science, and Technology of Japan and the Ministry of Health, Labour, and Welfare of Japan. This study was also supported by Joint Usage/Research Program of Medical Research Institute, Tokyo Medical and Dental University.

REFERENCES

Amali, A. A., Rekha, R. D., Lin, C. J., Wang, W. L., Gong, H. Y., Her, G. M. and Wu, J. L. (2006). Thioacetamide induced liver damage in zebrafish embryo as a disease model for steatohepatitis. *J. Biomed. Sci.* **13**, 225-232.

Aoki, K. and Matsudaira, H. (1977). Induction of hepatic tumors in a teleost (Oryzias latipes) after treatment with methylazoxymethanol acetate: brief communication. *J. Natl. Cancer Inst.* **59**, 1747-1749.

Balkan, J., Doğru-Abbasoğlu, S., Kanbağli, O., Cevikbaş, U., Aykaç-Toker, G. and Uysal, M. (2001). Taurine has a protective effect against thioacetamide-induced liver cirrhosis by decreasing oxidative stress. *Hum. Exp. Toxicol.* **20**, 251-254.

Balthasar, N., Dalgaard, L. T., Lee, C. E., Yu, J., Funahashi, H., Williams, T., Ferreira, M., Tang, V., McGovern, R. A., Kenny, C. D. et al. (2005). Divergence of melanocortin pathways in the control of food intake and energy expenditure. *Cell* **123**, 493-505.

Boorman, G. A., Botts, S., Bunton, T. E., Fournie, J. W., Harshbarger, J. C., Hawkins, W. E., Hinton, D. E., Jokinen, M. P., Okihiro, M. S. and Wolfe, M. J. (1997). Diagnostic criteria for degenerative, inflammatory, proliferative nonneoplastic and neoplastic liver lesions in medaka (Oryzias latipes): consensus of a National Toxicology Program Pathology Working Group. *Toxicol. Pathol.* **25**, 202-210.

Braunbeck, T., Görge, G., Storch, V. and Nagel, R. (1990). Hepatic steatosis in zebra fish (Brachydanio rerio) induced by long-term exposure to gamma-hexachlorocyclohexane. *Ecotoxicol. Environ. Saf.* **19**, 355-374.

Brown-Peterson, N. J., Krol, R. M., Zhu, Y. and Hawkins, W. E. (1999). N-nitrosodiethylamine initiation of carcinogenesis in Japanese medaka (Oryzias latipes): hepatocellular proliferation, toxicity, and neoplastic lesions resulting from short term, low level exposure. *Toxicol. Sci.* **50**, 186-194.

Brunt, E. M., Janney, C. G., Di Bisceglie, A. M., Neuschwander-Tetri, B. A. and Bacon, B. R. (1999). Nonalcoholic steatohepatitis: a proposal for grading and staging the histological lesions. *Am. J. Gastroenterol.* **94**, 2467-2474.

Bugianesi, E., Pagotto, U., Manini, R., Vanni, E., Gastaldelli, A., de Iasio, R., Gentilcore, E., Natale, S., Cassader, M., Rizzetto, M. et al. (2005). Plasma adiponectin in nonalcoholic fatty liver is related to hepatic insulin resistance and hepatic fat content, not to liver disease severity. *J. Clin. Endocrinol. Metab.* **90**, 3498-3504.

Bunton, T. E. (1990). Hepatopathology of diethylnitrosamine in the medaka (Oryzias latipes) following short-term exposure. *Toxicol. Pathol.* **18**, 313-323.

Capanni, M., Calella, F., Biagini, M. R., Genise, S., Raimondi, L., Bedogni, G., Svegliati-Baroni, G., Sofi, F., Milani, S., Abbate, R. et al. (2006). Prolonged n-3 polyunsaturated fatty acid supplementation ameliorates hepatic steatosis in patients with non-alcoholic fatty liver disease: a pilot study. *Aliment. Pharmacol. Ther.* **23**, 1143-1151.

Carten, J. D., Bradford, M. K. and Farber, S. A. (2011). Visualizing digestive organ morphology and function using differential fatty acid metabolism in live zebrafish. *Dev. Biol.* **360**, 276-285.

Chalasani, N., Deeg, M. A. and Crabb, D. W. (2004). Systemic levels of lipid peroxidation and its metabolic and dietary correlates in patients with nonalcoholic steatohepatitis. *Am. J. Gastroenterol.* **99**, 1497-1502.

Chalasani, N., Younossi, Z., Lavine, J. E., Diehl, A. M., Brunt, E. M., Cusi, K., Charlton, M. and Sanyal, A. J. (2012). The diagnosis and management of non-alcoholic fatty liver disease: practice Guideline by the American Association for the Study of Liver Diseases, American College of Gastroenterology, and the American Gastroenterological Association. *Hepatology* **55**, 2005-2023.

Chen, S. W., Chen, Y. X., Shi, J., Lin, Y. and Xie, W. F. (2006). The restorative effect of taurine on experimental nonalcoholic steatohepatitis. *Dig. Dis. Sci.* **51**, 2225-2234.

Cinaroglu, A., Gao, C., Imrie, D. and Sadler, K. C. (2011). Activating transcription factor 6 plays protective and pathological roles in steatosis due to endoplasmic reticulum stress in zebrafish. *Hepatology* **54**, 495-508.

Colak, Y., Ozturk, O., Senates, E., Tuncer, I., Yorulmaz, E., Adali, G., Doganay, L. and Enc, F. Y. (2011). SIRT1 as a potential therapeutic target for treatment of nonalcoholic fatty liver disease. *Med. Sci. Monit.* **17**, HY5-HY9.

Day, C. P. (2006). From fat to inflammation. *Gastroenterology* **130**, 207-210.

Day, C. P. and James, O. F. (1998). Steatohepatitis: a tale of two "hits"? *Gastroenterology* **114**, 842-845.

Deng, Q. G., She, H., Cheng, J. H., French, S. W., Koop, D. R., Xiong, S. and Tsukamoto, H. (2005). Steatohepatitis induced by intragastric overfeeding in mice. *Hepatology* **42**, 905-914.

Diehl, A. M. (2002). Nonalcoholic steatosis and steatohepatitis IV. Nonalcoholic fatty liver disease abnormalities in macrophage function and cytokines. *Am. J. Physiol. Gastrointest. Liver Physiol.* **282**, G1-G5.

Dixon, J. B. (2010). The effect of obesity on health outcomes. *Mol. Cell. Endocrinol.* **316**, 104-108.

Ekstedt, M., Franzén, L. E., Mathiesen, U. L., Thorelius, L., Holmqvist, M., Bodemar, G. and Kechagias, S. (2006). Long-term follow-up of patients with NAFLD and elevated liver enzymes. *Hepatology* **44**, 865-873.

Engelhard, Y. N., Gazer, B. and Paran, E. (2006). Natural antioxidants from tomato extract reduce blood pressure in patients with grade-1 hypertension: a double-blind, placebo-controlled pilot study. *Am. Heart J.* **151**, 100.

Goldsmith, J. R. and Jobin, C. (2012). Think small: zebrafish as a model system of human pathology. *J. Biomed. Biotechnol.* **2012**, 817341.

Gut, P., Baeza-Raja, B., Andersson, O., Hasenkamp, L., Hsiao, J., Hesselson, D., Akassoglou, K., Verdin, E., Hirschey, M. D. and Stainier, D. Y. (2013). Whole-organism screening for gluconeogenesis identifies activators of fasting metabolism. *Nat. Chem. Biol.* **9**, 97-104.

Hammes, T. O., Pedroso, G. L., Hartmann, C. R., Escobar, T. D., Fracasso, L. B., da Rosa, D. P., Marroni, N. P., Porawski, M. and da Silveira, T. R. (2012). The effect of taurine on hepatic steatosis induced by thioacetamide in zebrafish (Danio rerio). *Dig. Dis. Sci.* **57**, 675-682.

Her, G. M., Hsu, C. C., Hong, J. R., Lai, C. Y., Hsu, M. C., Pang, H. W., Chan, S. K. and Pai, W. Y. (2011). Overexpression of gankyrin induces liver steatosis in zebrafish (Danio rerio). *Biochim. Biophys. Acta* **1811**, 536-548.

Her, G. M., Pai, W. Y., Lai, C. Y., Hsieh, Y. W. and Pang, H. W. (2013). Ubiquitous transcription factor YY1 promotes zebrafish liver steatosis and lipotoxicity by inhibiting CHOP-10 expression. *Biochim. Biophys. Acta* **1831**, 1037-1051.

Higashitsuji, H., Itoh, K., Nagao, T., Dawson, S., Nonoguchi, K., Kido, T., Mayer, R. J., Arii, S. and Fujita, J. (2000). Reduced stability of retinoblastoma protein by gankyrin, an oncogenic ankyrin-repeat protein overexpressed in hepatomas. *Nat. Med.* **6**, 96-99.

Howarth, D. L., Vacaru, A. M., Tsedensodnom, O., Mormone, E., Nieto, N., Costantini, L. M., Snapp, E. L. and Sadler, K. C. (2012). Alcohol disrupts endoplasmic reticulum function and protein secretion in hepatocytes. *Alcohol. Clin. Exp. Res.* **36**, 14-23.

Huang, X. D., Fan, Y., Zhang, H., Wang, P., Yuan, J. P., Li, M. J. and Zhan, X. Y. (2008). Serum leptin and soluble leptin receptor in non-alcoholic fatty liver disease. *World J. Gastroenterol.* **14**, 2888-2893.

Huang, P., Zhu, Z., Lin, S. and Zhang, B. (2012). Reverse genetic approaches in zebrafish. *J. Genet. Genomics* **39**, 421-433.

Hugo, S. E., Cruz-Garcia, L., Karanth, S., Anderson, R. M., Stainier, D. Y. and Schlegel, A. (2012). A monocarboxylate transporter required for hepatocyte secretion of ketone bodies during fasting. *Genes Dev.* **26**, 282-293.

Ishikawa, T., Shimamine, T. and Takayama, S. (1975). Histologic and electron microscopy observations on diethylnitrosamine-induced hepatomas in small aquarium fish (Oryzias latipes). *J. Natl. Cancer Inst.* **55**, 909-916.

Itoh, M., Suganami, T., Nakagawa, N., Tanaka, M., Yamamoto, Y., Kamei, Y., Terai, S., Sakaida, I. and Ogawa, Y. (2011). Melanocortin 4 receptor-deficient mice as a novel mouse model of nonalcoholic steatohepatitis. *Am. J. Pathol.* **179**, 2454-2463.

Kleiner, D. E., Brunt, E. M., Van Natta, M., Behling, C., Contos, M. J., Cummings, O. W., Ferrell, L. D., Liu, Y. C., Torbenson, M. S., Unalp-Arida, A. et al.; Nonalcoholic Steatohepatitis Clinical Research Network (2005). Design and validation of a histological scoring system for nonalcoholic fatty liver disease. *Hepatology* **41**, 1313-1321.

Kuwashiro, S., Terai, S., Oishi, T., Fujisawa, K., Matsumoto, T., Nishina, H. and Sakaida, I. (2011). Telmisartan improves nonalcoholic steatohepatitis in medaka (Oryzias latipes) by reducing macrophage infiltration and fat accumulation. *Cell Tissue Res.* **344**, 125-134.

Lemoine, M., Ratziu, V., Kim, M., Maachi, M., Wendum, D., Paye, F., Bastard, J. P., Poupon, R., Housset, C., Capeau, J. et al. (2009). Serum adipokine levels predictive of liver injury in non-alcoholic fatty liver disease. *Liver Int.* **29**, 1431-1438.

Li, Z., Huang, X., Zhan, H., Zeng, Z., Li, C., Spitsbergen, J. M., Meierjohann, S., Schartl, M. and Gong, Z. (2012). Inducible and repressable oncogene-addicted hepatocellular carcinoma in Tet-on xmrk transgenic zebrafish. *J. Hepatol.* **56**, 419-425.

Li, Z., Zheng, W., Wang, Z., Zeng, Z., Zhan, H., Li, C., Zhou, L., Yan, C., Spitsbergen, J. M. and Gong, Z. (2013). A transgenic zebrafish liver tumor model with inducible Myc expression reveals conserved Myc signatures with mammalian liver tumors. *Dis. Model. Mech.* **6**, 414-423.

Lu, J. W., Yang, W. Y., Lin, Y. M., Jin, S. L. and Yuh, C. H. (2013). Hepatitis B virus X antigen and aflatoxin B1 synergistically cause hepatitis, steatosis and liver hyperplasia in transgenic zebrafish. *Acta Histochem.* (in press)

Matsumoto, T., Terai, S., Oishi, T., Kuwashiro, S., Fujisawa, K., Yamamoto, N., Fujita, Y., Hamamoto, Y., Furutani-Seiki, M., Nishina, H. et al. (2010). Medaka as a model for human nonalcoholic steatohepatitis. *Dis. Model. Mech.* **3**, 431-440.

Matteoni, C. A., Younossi, Z. M., Gramlich, T., Boparai, N., Liu, Y. C. and McCullough, A. J. (1999). Nonalcoholic fatty liver disease: a spectrum of clinical and pathological severity. *Gastroenterology* **116**, 1413-1419.

Matthews, R. P., Lorent, K., Mañoral-Mobias, R., Huang, Y., Gong, W., Murray, I. V., Blair, I. A. and Pack, M. (2009). TNFalpha-dependent hepatic steatosis and liver degeneration caused by mutation of zebrafish S-adenosylhomocysteine hydrolase. *Development* **136**, 865-875.

Menescal, L. A., Schmidt, C., Liedtke, D. and Schartl, M. (2012). Liver hyperplasia after tamoxifen induction of Myc in a transgenic medaka model. *Dis. Model. Mech.* **5**, 492-502.

Mensenkamp, A. R., van Luyn, M. J., van Goor, H., Bloks, V., Apostel, F., Greeve, J., Hofker, M. H., Jong, M. C., van Vlijmen, B. J., Havekes, L. M. et al. (2000). Hepatic lipid accumulation, altered very low density lipoprotein formation and apolipoprotein E deposition in apolipoprotein E3-Leiden transgenic mice. *J. Hepatol.* **33**, 189-198.

Miyake, A., Higashijima, S., Kobayashi, D., Narita, T., Jindo, T., Setiamarga, D. H., Ohisa, S., Orihara, N., Hibiya, K., Konno, S. et al. (2008). Mutation in the abcb7 gene causes abnormal iron and fatty acid metabolism in developing medaka fish. *Dev. Growth Differ.* **50**, 703-716.

Monk, K. R., Voas, M. G., Franzini-Armstrong, C., Hakkinen, I. S. and Talbot, W. S. (2013). Mutation of sec63 in zebrafish causes defects in myelinated axons and liver pathology. *Dis. Model. Mech.* **6**, 135-145.

Nagarajan, P., Mahesh Kumar, M. J., Venkatesan, R., Majundar, S. S. and Juyal, R. C. (2012). Genetically modified mouse models for the study of nonalcoholic fatty liver disease. *World J. Gastroenterol.* **18**, 1141-1153.

Neuschwander-Tetri, B. A. and Caldwell, S. H. (2003). Nonalcoholic steatohepatitis: summary of an AASLD Single Topic Conference. *Hepatology* **37**, 1202-1219.

Nguyen, A. T., Emelyanov, A., Koh, C. H., Spitsbergen, J. M., Lam, S. H., Mathavan, S., Parinov, S. and Gong, Z. (2011). A high level of liver-specific expression of oncogenic Kras(V12) drives robust liver tumorigenesis in transgenic zebrafish. *Dis. Model. Mech.* **4**, 801-813.

Nguyen, A. T., Emelyanov, A., Koh, C. H., Spitsbergen, J. M., Parinov, S. and Gong, Z. (2012). An inducible kras(V12) transgenic zebrafish model for liver tumorigenesis and chemical drug screening. *Dis. Model. Mech.* **5**, 63-72.

Oishi, T., Terai, S., Kuwashiro, S., Fujisawa, K., Matsumoto, T., Nishina, H. and Sakaida, I. (2012). Ezetimibe reduces fatty acid quantity in liver and decreased inflammatory cell infiltration and improved NASH in medaka model. *Biochem. Biophys. Res. Commun.* **422**, 22-27.

Oka, T., Nishimura, Y., Zang, L., Hirano, M., Shimada, Y., Wang, Z., Umemoto, N., Kuroyanagi, J., Nishimura, N. and Tanaka, T. (2010). Diet-induced obesity in zebrafish shares common pathophysiological pathways with mammalian obesity. *BMC Physiol.* **10**, 21.

Pai, W. Y., Hsu, C. C., Lai, C. Y., Chang, T. Z., Tsai, Y. L. and Her, G. M. (2013). Cannabinoid receptor 1 promotes hepatic lipid accumulation and lipotoxicity through the induction of SREBP-1c expression in zebrafish. *Transgenic Res.* (in press)

Passeri, M. J., Cinaroglu, A., Gao, C. and Sadler, K. C. (2009). Hepatic steatosis in response to acute alcohol exposure in zebrafish requires sterol regulatory element binding protein activation. *Hepatology* **49**, 443-452.

Pessayre, D. and Fromenty, B. (2005). NASH: a mitochondrial disease. *J. Hepatol.* **42**, 928-940.

Postic, C. and Girard, J. (2008). Contribution of de novo fatty acid synthesis to hepatic steatosis and insulin resistance: lessons from genetically engineered mice. *J. Clin. Invest.* **118**, 829-838.

Puri, P., Mirshahi, F., Cheung, O., Natarajan, R., Maher, J. W., Kellum, J. M. and Sanyal, A. J. (2008). Activation and dysregulation of the unfolded protein response in nonalcoholic fatty liver disease. *Gastroenterology* **134**, 568-576.

Rekha, R. D., Amali, A. A., Her, G. M., Yeh, Y. H., Gong, H. Y., Hu, S. Y., Lin, G. H. and Wu, J. L. (2008). Thioacetamide accelerates steatohepatitis, cirrhosis and HCC by expressing HCV core protein in transgenic zebrafish Danio rerio. *Toxicology* **243**, 11-22.

Sadler, K. C., Amsterdam, A., Soroka, C., Boyer, J. and Hopkins, N. (2005). A genetic screen in zebrafish identifies the mutants vps18, nf2 and foie gras as models of liver disease. *Development* **132**, 3561-3572.

Sanyal, A. J., Campbell-Sargent, C., Mirshahi, F., Rizzo, W. B., Contos, M. J., Sterling, R. K., Luketic, V. A., Shiffman, M. L. and Clore, J. N. (2001). Nonalcoholic steatohepatitis: association of insulin resistance and mitochondrial abnormalities. *Gastroenterology* **120**, 1183-1192.

Schlegel, A. and Stainier, D. Y. (2007). Lessons from "lower" organisms: what worms, flies, and zebrafish can teach us about human energy metabolism. *PLoS Genet.* **3**, e199.

Schwarz, J. M., Linfoot, P., Dare, D. and Aghajanian, K. (2003). Hepatic de novo lipogenesis in normoinsulinemic and hyperinsulinemic subjects consuming high-fat, low-carbohydrate and low-fat, high-carbohydrate isoenergetic diets. *Am. J. Clin. Nutr.* **77**, 43-50.

Scrivens, P. J., Noueihed, B., Shahrzad, N., Hul, S., Brunet, S. and Sacher, M. (2011). C4orf41 and TTC-15 are mammalian TRAPP components with a role at an early stage in ER-to-Golgi trafficking. *Mol. Biol. Cell* **22**, 2083-2093.

Sekiya, M., Yahagi, N., Matsuzaka, T., Najima, Y., Nakakuki, M., Nagai, R., Ishibashi, S., Osuga, J., Yamada, N. and Shimano, H. (2003). Polyunsaturated fatty acids ameliorate hepatic steatosis in obese mice by SREBP-1 suppression. *Hepatology* **38**, 1529-1539.

Shieh, Y. S., Chang, Y. S., Hong, J. R., Chen, L. J., Jou, L. K., Hsu, C. C. and Her, G. M. (2010). Increase of hepatic fat accumulation by liver specific expression of Hepatitis B virus X protein in zebrafish. *Biochim. Biophys. Acta* **1801**, 721-730.

Steiling, H., Wüstefeld, T., Bugnon, P., Brauchle, M., Fässler, R., Teupser, D., Thiery, J., Gordon, J. I., Trautwein, C. and Werner, S. (2003). Fibroblast growth factor receptor signalling is crucial for liver homeostasis and regeneration. *Oncogene* **22**, 4380-4388.

Stewart, S. T., Cutler, D. M. and Rosen, A. B. (2009). Forecasting the effects of obesity and smoking on U.S. life expectancy. *N. Engl. J. Med.* **361**, 2252-2260.

Tainaka, T., Shimada, Y., Kuroyanagi, J., Zang, L., Oka, T., Nishimura, Y., Nishimura, N. and Tanaka, T. (2011). Transcriptome analysis of anti-fatty liver action by Campari tomato using a zebrafish diet-induced obesity model. *Nutr. Metab. (Lond)* **8**, 88.

Tanaka, N., Sano, K., Horiuchi, A., Tanaka, E., Kiyosawa, K. and Aoyama, T. (2008). Highly purified eicosapentaenoic acid treatment improves nonalcoholic steatohepatitis. *J. Clin. Gastroenterol.* **42**, 413-418.

Thakur, P. C., Stuckenholz, C., Rivera, M. R., Davison, J. M., Yao, J. K., Amsterdam, A., Sadler, K. C. and Bahary, N. (2011). Lack of de novo phosphatidylinositol synthesis leads to endoplasmic reticulum stress and hepatic steatosis in cdipt-deficient zebrafish. *Hepatology* **54**, 452-462.

Tomita, K., Oike, Y., Teratani, T., Taguchi, T., Noguchi, M., Suzuki, T., Mizutani, A., Yokoyama, H., Irie, R., Sumimoto, H. et al. (2008). Hepatic AdipoR2 signaling plays a protective role against progression of nonalcoholic steatohepatitis in mice. *Hepatology* **48**, 458-473.

Tsai, S. M., Liu, D. W. and Wang, W. P. (2013). Fibroblast growth factor (Fgf) signaling pathway regulates liver homeostasis in zebrafish. *Transgenic Res.* **22**, 301-314.

van der Velden, Y. U., Wang, L., Zevenhoven, J., van Rooijen, E., van Lohuizen, M., Giles, R. H., Clevers, H. and Haramis, A. P. (2011). The serine-threonine kinase LKB1 is essential for survival under energetic stress in zebrafish. *Proc. Natl. Acad. Sci. USA* **108**, 4358-4363.

Wang, Y., Ausman, L. M., Greenberg, A. S., Russell, R. M. and Wang, X. D. (2010). Dietary lycopene and tomato extract supplementations inhibit nonalcoholic steatohepatitis-promoted hepatocarcinogenesis in rats. *Int. J. Cancer* **126**, 1788-1796.

Whitehead, J. P., Richards, A. A., Hickman, I. J., Macdonald, G. A. and Prins, J. B. (2006). Adiponectin—a key adipokine in the metabolic syndrome. *Diabetes Obes. Metab.* **8**, 264-280.

Xu, A., Wang, Y., Keshaw, H., Xu, L. Y., Lam, K. S. and Cooper, G. J. (2003). The fat-derived hormone adiponectin alleviates alcoholic and nonalcoholic fatty liver diseases in mice. *J. Clin. Invest.* **112**, 91-100.

Yee, N. S., Lorent, K. and Pack, M. (2005). Exocrine pancreas development in zebrafish. *Dev. Biol.* **284**, 84-101.

脳における SAPK/JNK シグナルの役割

山崎 世和　仁科 博史

はじめに

多様なストレスによって活性化されるストレス応答性 MAP キナーゼ(stress-activated protein kinase：SAPK)は，転写因子 c-Jun の N 末端をリン酸化する酵素(c-Jun N-terminal kinase：JNK)としてよく知られている．哺乳動物には JNK をコードする遺伝子が 3 種類存在しており，JNK1，2 はほとんど全ての組織で発現しているのに対し，JNK3 は脳や精巣に発現が限局されている．活性化された JNK は様々な標的タンパク質をリン酸化することで，遺伝子発現や細胞の生死などの細胞応答を引きおこすことが報告されている[1,2]．

JNK は，活性化ループに存在するスレオニン-プロリン-チロシン配列のスレオニンとチロシンが，MAP キナーゼキナーゼ(MAPKK)である MKK4 と MKK7 によってリン酸化され，活性化される．MKK4，MKK7 はともにセリン/スレオニンおよびチロシンのリン酸化活性を持つ二重特異性リン酸化酵素(dual specificity kinase)である．MKK4 と MKK7 の活性化はさらに上流の MAP キナーゼキナーゼキナーゼ(MAPKKK)によって制御されており，dual leucine zipper kinase (DLK)，apoptosis signal-regulating kinase (ASK)，mixed lineage protein kinase (MLK)など 10 種類以上が同定されている．

JNK シグナルの活性化は JNK-interacting protein (JIP) 1，JIP2，JIP3 などの足場タンパク質によっても制御される．これらの足場タンパク質は MAPKKK，MAPKK，MAPK と結合することで酵素複合体を形成し，シグナルの伝達効率を調節する．また，複合体に会合する酵素を使い分けることでシグナルに特異性と多様性を持たせていると考えられている．

哺乳動物では，多くの組織において JNK の活性は定常状態で低いレベルに保たれているが，脳においては恒常的に高い JNK の活性化を観察することができる．これまで JNK や MKK の遺伝子欠損マウスを用いた研究によって，この恒常的活性化が脳において神経細胞移動や軸索形成などに関与することが示されている[3](図)．次項からはこれらの表現型を通して JNK シグナルの脳における役割を概説する．

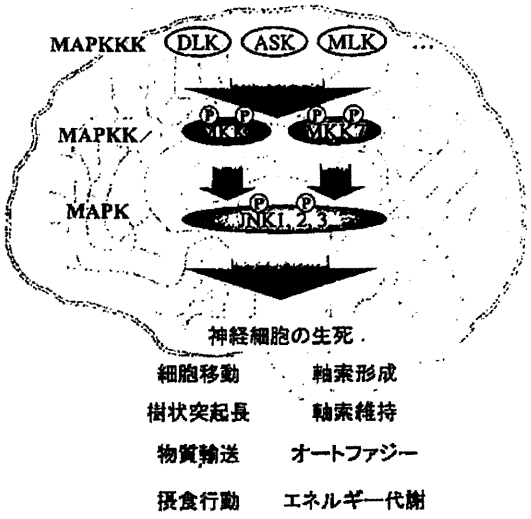

哺乳動物の脳における JNK シグナル経路

DLK，ASK，MLK などの MAPKKK が MAPKK である MKK4，MKK7 をリン酸化(P)し，それらが JNK1，2，3 をリン酸化する．リン酸化され活性化された JNK は脳において様々な現象を制御する．

Jnk 欠損マウスの表現型

1．*Jnk* 単独欠損マウス

JNK1，2，3 をコードする各遺伝子の全身性単独欠損(KO)マウスがこれまで作出されているが，いずれにおいても致死を引きおこすような重篤な異常は観察されていない．しかし詳細な解析によって興味深い表現型が見出されている(表 1)．*Jnk1* KO マウスを用いた研究によって，① 大脳皮質で産生された神経細胞の放射状移動が野生型に比べて早くなり，それに伴って皮質板が肥厚し脳室帯が薄層化すること，② 大脳交連(脳梁，前交連，海馬交連)などの軸索路形成に異常は観察されないが，前交連が生後徐々に消失していくこと，③ 運動皮質の神経細胞において 150 μm 以下の短い樹状突起の割合が野生型に比べて顕著に増加することが示された[4~6]．これらの結果から，JNK1 は脳の正常な形態形成に必須であることが明らかとなっている．

やまさき ときわ　東京医科歯科大学難治疾患研究所/発生再生生物学分野
にしな ひろし　同 教授

0289-0585/13/¥500/論文/JCOPY

成体マウスの脳室にホルモンを投与し摂食行動を検討する実験において，野生型でおこるグルココルチコイドやインスリンに応答した摂食量の変化が，*Jnk1* KO マウスでは増強されることが示された[7]．肝臓や脂肪組織などの主要な代謝組織における JNK 欠損の影響を排除するため，神経系特異的 *Jnk1* 欠損(*Jnk1* cKO)マウスが作出された．本マウスに高脂肪食付加を行ったところ，野生型と比較してインスリン抵抗性やグルコース代謝異常が改善し，肝脂肪変性や脂肪組織の機能異常が抑制された[8]．これらの報告から，JNK1 は脳による摂食行動やエネルギー代謝の制御に関与することが示されている．

パーキンソン病モデル作製に使用される 1-methyl-4-phenyl-1, 2, 3, 6-tetrahydropyridine(MPTP)は中脳黒質緻密部においてドーパミン作動性神経の変性を誘導するが，*Jnk2* KO, *Jnk3* KO マウスでは MPTP 投与による神経細胞死が野生型に比べて顕著に抑制された[9]．また *Jnk3* KO マウスでは，カイニン酸による興奮毒性や脳虚血などによって誘導される細胞死も抑制された[10~13]．これらの結果から，JNK2, JNK3 は神経毒やストレスに応答し細胞死を誘導する機能を持つと考えられる．

2．*Jnk* 二重欠損マウス

Jnk1/2 二重欠損(DKO)マウスは神経管閉鎖異常を伴い生後 11～12 日に致死となった[14,15]．神経管の TUNEL 染色から，野生型に比べて前脳では細胞死が亢進すること，後脳では細胞死が抑制されることが示された．また，*Jnk1* ヘテロ欠損と *Jnk2* KO(*Jnk1*+/− *Jnk2*−/−)マウスでは発生異常が観察されないのに対し，*Jnk1* KO と *Jnk2* ヘテロ欠損(*Jnk1*−/− *Jnk2*+/−)マウスにおいて約 25%の個体で神経管閉鎖異常に起因する外脳症の表現型がみられた．*Jnk2/3* DKO マウスについては発生は正常に進み脳の形態異常も報告されていないが，MPTP 投与による神経細胞死が単独 KO より強く抑制され，パーキンソン病様の運動失調も有意に改善することが示された[9]．これらの結果から，JNK シグナルが神経細胞死を正にも負にも制御すること，JNK1, 2, 3 の間には相補的な機能が存在することが示唆される．

3．*Jnk1/2/3* 三重欠損マウス

JNK1, 2, 3 の相補的な機能を排除するため，JNK の全ての遺伝子を条件付きに欠損(*Jnk1/2/3* cTKO)させた神経細胞およびマウスが作出された[16]．JNK を全て欠損させた小脳顆粒細胞の初代培養において，① 軸索が肥大すること，② 神経細胞の寿命が延長すること，③ ミトコンドリアやシナプス小胞，リソソームが蓄積すること，④ ライブイメージングでミトコンドリアの輸送障害が観察されること，⑤ オートファジーが亢進することが示された．また，個体レベルの解析を行うため神経幹細胞で Cre が発現する *Nestin-Cre* を用いた *Jnk1/2/3* cTKO マウスが作出されたが，胎生初期に致死となった．そこで小脳 Purkinje 細胞特異的 *Pcp2-Cre* を用いて，致死を回避する *Jnk1/2/3* cTKO マウスが作出された．本マウスの小脳を免疫染色や電子顕微鏡によって解析したところ，軸索の肥大やミトコンドリアの局在異常，オートファジーの亢進など，初代培養細胞の系でみられた表現型が同様に観察された．このように JNK1, 2, 3 全てを欠損させることで，JNK シグナルが神経細胞において物質輸送やオートファジーを制御することが明らかとなった．

表 1　*Jnk* 欠損マウスの表現型

遺伝子欠損マウス	表現型	文献
Jnk1 KO	大脳皮質神経細胞の放射状移動の加速 樹状突起数の増加 前交連の維持異常 摂食行動における糖質コルチコイド，インスリンの影響の増強	4-7
Jnk1 cKO (*Nestin-Cre*)	高脂肪食誘導性の耐糖能異常とインスリン抵抗性の改善 インスリン様成長因子，成長ホルモン，甲状腺ホルモンの血清濃度低下	8
Jnk2 KO	MPTP 誘導性神経細胞死への抵抗性増加	9
Jnk3 KO	MPTP 誘導性神経細胞死への抵抗性増加 カイニン酸誘導性神経細胞死への抵抗性増加 虚血誘導性神経細胞死への抵抗性増加 6-hydroxydopamine 誘導性神経細胞死への抵抗性増加	9-13
Jnk1/2 DKO	E11.5 における胎生致死 神経管閉鎖異常 前脳における細胞死の増加 後脳における細胞死の減少	14, 15
Jnk2/3 DKO	MPTP 誘導性神経細胞死への抵抗性増加	9
Jnk1/2/3 TKO (*Nestin-Cre*)	早期胎生致死	16
Jnk1/2/3 TKO (*Pcp2-Cre*)	軸索の肥大 ミトコンドリアの局在異常 オートファジーの亢進	16

MKK 欠損マウスの表現型

MKK4, 7 をコードする各遺伝子の KO マウス，DKO マウスの作出によって，JNK の活性化が初期胚の形態形成や器官発生に必須であることが明らかにされてきた[17]．一方で，これらのマウスは脳形成以前の胎生 10～12 日に致死となるため，MKK4, 7 の脳における機能については不明なままであった．近年になって *Nestin-Cre* を用いた cKO マウスが作出され，MKK4, 7 が脳発生において重要な役割を持つことが明らかにされた(表 2)．

1．*Mkk4* 条件付欠損マウス

MKK4 の脳における機能を検討するため，*Nestin-Cre*

表 2　*Mkk4* cKO マウスと *Mkk7* cKO マウスの表現型の違い

表現型	*Mkk4* cKO[18] (*Nestin-Cre*)	*Mkk7* cKO[19] (*Nestin-Cre*)
JNK 活性化	20%まで低下 (基質リン酸化活性)	20%まで低下 (JNK リン酸化量)
致死の時期	生後 3 週齢	出生直後
神経細胞移動	大脳皮質の放射状移動遅延 小脳 Purkinje 細胞の配置異常	大脳皮質の放射状移動遅延
軸索	前交連・脳梁が形成後に消失、(維持異常)	前交連・脳梁の形成異常
超微細構造の異常	報告なし	オートファゴソームの蓄積 ファイバー構造の蓄積
基質リン酸化	MAP1B リン酸化低下	MAP1B および DCX のリン酸化低下

を用いた *Mkk4* cKO マウスが作出された[18]．本マウスでは，① JNK の酵素活性が 20%まで低下すること，② 生後 2，3 日で成長が停止し 3 週間以降に死亡すること，③ 大脳皮質において神経細胞の放射状移動が遅延すること，④ 小脳 Purkinje 細胞の配置が乱れること，⑤ 一度形成された脳梁と前交連が 3 週齢ごろに消失すること，⑥ 微小管関連タンパク質(microtubule-associated protein：MAP)である MAP1B のリン酸化が低下することが示された．これらの結果から，*Mkk4* cKO マウスでは MAP のリン酸化低下による微小管ダイナミクスの破綻が，上記の表現型を引きおこしていると考えられる．

2．*Mkk7* 条件付欠損マウス

MKK7 についても *Nestin-Cre* を用いた条件付欠損(*Mkk7* cKO)マウスが作出された[19]．その結果，① JNK のリン酸化が 20%まで低下すること，② 出生直後に呼吸不全を伴って致死となること，③ 大脳皮質の神経細胞の放射状移動が遅延すること，④ オートファジーやファイバー構造が蓄積すること，⑤ 脳梁・前交連が形成されないこと，⑥ MAP1B に加え doublecortin(DCX)のリン酸化も顕著に低下することが観察された．

Mkk7 cKO マウスでは，*Mkk4* cKO マウスより早期に致死となるなど重篤な表現型が観察された．また，*Mkk7* cKO マウスでは軸索の形成に異常が観察されるのに対し，*Mkk4* cKO マウスは形成後の維持に異常を示した．これらの表現型の違いは，MKK4-JNK シグナルと MKK7-JNK シグナルの足場タンパク質や標的タンパク質の違いに起因すると考えられる．

むすび

JNK1，2，3，MKK4，7 の各遺伝子欠損マウスの作出によって，JNK シグナルが神経細胞の生死や脳発生の制御，および個体の恒常性維持に必須な役割を持つことが明らかとなった．また近年になって，ヒトの統合失調症患者で *mkk7* の mRNA 量が低下していることや *Mkk7* ヘテロ欠損マウスが作業記憶の障害を示すことが報告され，精神疾患における JNK シグナルの関与が注目されつつある[20]．今後は認知や記憶，精神活動など高次の脳機能における役割について研究が展開されることが期待される．

文　献

1) Davis RJ. Signal transduction by the JNK group of MAP kinases. Cell. 2000；103：239-52.
2) Chang L, Karin M. Mammalian MAP kinase signalling cascades. Nature. 2001；410：37-40.
3) Yamasaki T, Kawasaki H, Nishina H. Diverse roles of JNK and MKK pathways in the brain. J Signal Transduct. 2012：2012：459265.
4) Westerlund N, Zdrojewska J, Padzik A, et al. Phosphorylation of SCG10/stathmin-2 determines multipolar stage exit and neuronal migration rate. Nature Neurosci. 2011；14：305-13.
5) Björkblom B, Östman N, Hongisto V, et al. Constitutively active cytoplasmic c-Jun N-terminal kinase 1 is a dominant regulator of dendritic architecture：role of microtubule associated protein 2 as an effector. J Neurosci. 2005；25：6350-61.
6) Chang L, Jones Y, Ellisman MH, et al. JNK1 is required for maintenance of neuronal microtubules and controls phosphorylation of microtubule associated proteins. Dev Cell. 2003；4：521-33.
7) Unger EK, Piper ML, Olofsson LE, et al. Functional role of c-Jun-N-terminal kinase in feeding regulation. Endocrinology. 2010；151：671-82.
8) Belgardt BF, Mauer J, Wunderlich FT, et al. Hypothalamic and pituitary c-Jun N-terminal kinase 1 signaling coordinately regulates glucose metabolism. Proc Natl Acad Sci USA. 2010；107：6028-33.
9) Hunot S, Vila M, Teismann P, et al. JNK-mediated induction of cyclooxygenase 2 is required for neurodegeneration in a mouse model of Parkinson's disease. Proc Natl Acad Sci USA. 2004；101：665-70.
10) Yang DD, Kuan CY, Whitmarsh AJ, et al. Absence of excitotoxicity-induced apoptosis in the hippocampus of mice lacking the Jnk3 gene. Nature. 1997；389：865-70.
11) Kuan CY, Whitmarsh AJ, Yang DD, et al. A critical role of neural-specific JNK3 for ischemic apoptosis. Proc Natl Acad Sci USA. 2003；100：15184-9.
12) Pirianov G, Brywe KG, Mallard C, et al. Deletion of the c-Jun N-terminal kinase 3 gene protects neonatal mice against cerebral hypoxic-ischaemic injury. J Cereb Blood Flow Metab. 2007；27：1022-32.
13) Brecht S, Kirchhof R, Chromik A, et al. Specific pathophysiological functions of JNK isoforms in the brain. Eur J Neurosci. 2005；21：363-77.
14) Kuan CY, Yang DD, Samanta Roy DR, et al. The Jnk1 and Jnk2 protein kinases are required for regional specific apoptosis during early brain development. Neuron. 1999；22：667-76.
15) Sabapathy K, Jochum W, Hochedlinger K, et al. Defective neural tube morphogenesis and altered apoptosis in the absence of both JNK1 and JNK2. Mech Dev. 1999；89：115-24.
16) Xu P, Das M, Reilly J, et al. JNK regulates FoxO-dependent autophagy in neurons. Genes Dev. 2011；25：310-22.
17) Asaoka Y, Nishina H. Diverse physiological functions of MKK4 and MKK7 during early embryogenesis. J Biochem. 2010；148：393-401.
18) Wang X, Nadarajah B, Robinson AC, et al. Targeted deletion of the mitogen-activated protein kinase kinase 4 gene in the nervous system causes severe brain developmental defects and premature death. Mol Cell Biol. 2007；27：7935-46.
19) Yamasaki T, Kawasaki H, Arakawa S, et al. Stress-activated protein kinase MKK7 regulates axon elongation in the developing cerebral cortex. J Neurosci. 2011；31：16872-83.
20) Winchester CL, Ohzeki H, Vouyiouklis DA, et al. Converging evidence that sequence variations in the novel candidate gene MAP2K7 (MKK7) are functionally associated with schizophrenia. Hum Mol Genet. 2012；21：4910-21.

Hepatic Crown-Like Structure: A Unique Histological Feature in Non-Alcoholic Steatohepatitis in Mice and Humans

Michiko Itoh[1☯], Hideaki Kato[2,4☯], Takayoshi Suganami[1,3*], Kuniha Konuma[2], Yoshio Marumoto[5], Shuji Terai[5], Hiroshi Sakugawa[6], Sayaka Kanai[2], Miho Hamaguchi[2], Takahiro Fukaishi[2], Seiichiro Aoe[7], Kazunari Akiyoshi[8], Yoshihiro Komohara[9], Motohiro Takeya[9], Isao Sakaida[5], Yoshihiro Ogawa[2*]

1 Department of Organ Network and Metabolism, Tokyo Medical and Dental University, Tokyo, Japan, **2** Department of Molecular Endocrinology and Metabolism, Graduate School of Medical and Dental Sciences, Tokyo Medical and Dental University, Tokyo, Japan, **3** Japan Science and Technology Agency, PRESTO, Tokyo, Japan, **4** Medical Research Laboratories, Shionogi & Co. Ltd., Osaka, Japan, **5** Department of Gastroenterology and Hepatology, Yamaguchi University Graduate School of Medicine, Yamaguchi, Japan, **6** Heart Life Hospital, Okinawa, Japan, **7** Department of Home Economics, Otsuma Women's University, Tokyo, Japan, **8** Department of Polymer Chemistry, Kyoto University Graduate School of Engineering, Kyoto, Japan, **9** Department of Cell Pathology, Graduate School of Medical Sciences, Kumamoto University, Kumamoto, Japan

Abstract

Although macrophages are thought to be crucial for the pathogenesis of chronic inflammatory diseases, how they are involved in disease progression from simple steatosis to non-alcoholic steatohepatitis (NASH) is poorly understood. Here we report the unique histological structure termed "hepatic crown-like structures (hCLS)" in the mouse model of human NASH; melanocortin-4 receptor deficient mice fed a Western diet. In hCLS, CD11c-positive macrophages aggregate to surround hepatocytes with large lipid droplets, which is similar to those described in obese adipose tissue. Histological analysis revealed that hCLS is closely associated with activated fibroblasts and collagen deposition. When treatment with clodronate liposomes effectively depletes macrophages scattered in the liver, with those in hCLS intact, hepatic expression of inflammatory and fibrogenic genes is unaffected, suggesting that hCLS is an important source of inflammation and fibrosis during the progression of NASH. Notably, the number of hCLS is positively correlated with the extent of liver fibrosis. We also observed increased number of hCLS in the liver of non-alcoholic fatty liver disease/NASH patients. Collectively, our data provide evidence that hCLS is involved in the development of hepatic inflammation and fibrosis, thereby suggesting its pathophysiologic role in disease progression from simple steatosis to NASH.

Citation: Itoh M, Kato H, Suganami T, Konuma K, Marumoto Y, et al. (2013) Hepatic Crown-Like Structure: A Unique Histological Feature in Non-Alcoholic Steatohepatitis in Mice and Humans. PLoS ONE 8(12): e82163. doi:10.1371/journal.pone.0082163

Editor: Silvia C. Sookoian, Institute of Medical Research A Lanari-IDIM, University of Buenos Aires-National Council of Scientific and Technological Research (CONICET), Argentina

Received August 1, 2013; **Accepted** October 21, 2013; **Published** December 11, 2013

Funding: This work was supported in part by Grants-in-Aid for Scientific Research from the Ministry of Education, Culture, Sports, Science and Technology of Japan, the Ministry of Health, Labour and Welfare of Japan, and Japan Science and Technology Agency, PRESTO. This work was also supported by research grants from Takeda Science Foundation, Ono Medical Research Foundation, Japan Research Foundation for Clinical Pharmacology, Nestlé Nutrition Council, Japan, Astellas Foundation for Research on Metabolic Disorders, The Uehara Memorial Foundation, and the Joint Usage/Research Program of Medical Research Institute, Tokyo Medical and Dental University. The funders had no role in study design, data collection and analysis, decision to publish, or preparation of the manuscript.

Competing Interests: HK is an employee of Shionogi & Co. Ltd. The authors have declared that no competing interests exist. This does not alter the authors' adherence to all the PLOS ONE policies on sharing data and materials.

* E-mail: ogawa.mem@tmd.ac.jp (YO); suganami.mem@tmd.ac.jp (TS)

☯ These authors contributed equally to this work.

Introduction

Non-alcoholic fatty liver disease (NAFLD) is one of the most common forms of chronic liver disease closely related to the metabolic syndrome and type 2 diabetes mellitus [1,2]. The clinical spectrum of NAFLD ranges from simple hepatic steatosis to non-alcoholic steatohepatitis (NASH), the latter of which can progress to cirrhosis and hepatocellular carcinoma [3]. According to the "two-hit" hypothesis, the pathogenesis of NASH may involve at least two processes; excessive accumulation of lipids in the liver as the 1st hit plus additional pathogenic stimuli as the 2nd hit, such as proinflammatory cytokines, oxidative stress, endotoxins, and lipotoxicity [4,5,6,7]. Hepatic macrophages are a major source of proinflammatory mediators such as tumor necrosis factor-α (TNFα), interleukin-6, and reactive oxygen species, which are considered to accelerate hepatic steatosis and insulin resistance [8,9]. There is evidence that macrophages are involved in the pathogenesis of some rodent models of experimentally-induced liver fibrosis [10,11]. However, the pathophysiologic role of macrophages in the development of NASH is still unclear; it is partly because the limited availability of suitable animal models that reflect a liver condition of human NASH [12]. For instance, chemically-induced liver fibrosis is not accompanied by obesity, insulin resistance, and hepatic steatosis [12]. Dietary deficiency of methionine and choline also develops steatosis and mild fibrosis, without obesity and insulin resistance [12].

We have recently reported that melanocortin-4 receptor (MC4R) deficient (MC4R-KO) mice on a high-fat diet (HFD)